NMR Approach to Probe Protein-Protein Interactions Using ^{13}C-Methylation of Lysine Residues

（リジン残基の ^{13}C メチル化を用いたNMRによるタンパク質間相互作用検出）

服部 良一

大阪大学大学院理学研究科化学専攻
（蛋白質研究所機能構造計測学研究室）

Contents

Abbreviations

NMR	nuclear magnetic resonance
PDB	protein data bank
HSQC	heteronuclear single quantum correlation
NOE	nuclear Overhauser effect
E. coli	*Escherichia coli*
K_d	dissociation constant
UBA	ubiquitin-associated
GST	glutathione S-transferase
HRV3C	human rhinovirus 3C
OD_{600}	optical density at 600 nm
IPTG	isopropyl-b-D-thiogalactopyranoside
Tris	tris(hydroxymethyl)aminomethane
DTT	dithiothreitol
EDTA	ethylenediaminetetraacetic acid
$Dsk2_{UBA}$	UBA domain of *yeast* Dsk2
UV-Vis	ultraviolet-visible
$p62_{UBA}$	UBA domain of *mouse* p62
FKBP12	12 kDa FK506-binding protein
DMAB	dimethylamine borane
MALDI-MS	matrix assisted laser desorption/ionization-mass spectrometry
DSS	2,2-dimethyl-2-silapentane-5-sulfonic acid
ITC	isothermal titration calorimetry
RMSD	root-mean-square deviation
UBQ	methylated ubiquitin
FKBP	methylated FKBP12
TRX	methylated thioredoxin

1. Introduction

1.1. Isotope Labeling of Proteins

Nuclear Magnetic Resonance (NMR) spectroscopy is a powerful method for obtaining structural information of biological macromolecules under physiological conditions at atomic resolution. NMR has become an established method for solving protein structures as over 9000 NMR structures were deposited to Protein Data Bank (PDB) to date (January 2014). Moreover, recent progress in protein NMR analysis has been made not only for structural determination but also dynamics and molecular interactions. These achievements would not have been possible without the development of isotope labeling methods (1).

Stable isotope, such as NMR active ^{13}C and ^{15}N, labeling is essential for current NMR measurements of proteins. This is because the protein has too many ^{1}H atoms to be resolved in the ^{1}H NMR spectrum. The isotope labeling makes the resonances of many ^{1}H atoms possible to resolve using heteronuclear NMR measurements, such as ^{1}H-^{13}C and ^{1}H-^{15}N heteronuclear single quantum correlation (HSQC). The resonance assignments are performed by ^{1}H-^{13}C-^{15}N triple resonance measurements utilizing many kinds of through-bond spin-spin couplings (2). The resonance assignments enable to analyze a huge number of ^{1}H-^{1}H nuclear Overhauser effects (NOEs) that correlate inter-atom distances. Nowadays, structure determination of proteins with molecular weight up to 30 kDa is available with the aid of sophisticated computational methods (3). Furthermore, deuteration and site-specific labeling techniques are utilized to enhance sensitivity and to resolve overlapping peaks. These techniques enable to analyze the dynamics and molecular interactions of larger proteins with molecular weight beyond 50 kDa, and protein complexes with molecular weight of several hundred kDa (4,5).

The isotope labeling of proteins is generally performed using recombinant *Escherichia*

coli (*E. coli*) expression system due to the advantages in handling, growth rate and labeling cost. However, difficulties may be encountered in obtaining sufficient protein expression, maintaining protein solubility and functional structure. In recent years, isotope labeling techniques using non-*E. coli* prokaryotic or eukaryotic cells, which are effective for the protein production requiring disulfide-bond formation and post-translational modifications, has been developed (6). These techniques are useful but several drawbacks in terms of yield and cost still exist. On the other hand, chemical attachment of isotope labeled moieties to the reactive groups in proteins can be an alternative approach of isotope labeling. The labeling strategy using chemical modification is easy to apply to most proteins, because purified proteins without isotope-labeled, even from organisms, can be used for isotope labeling (Figure 1.1).

1.2. ^{13}C-Methylation of Lysine Residues

Amino group in lysine residues is a functional group frequently targeted in the chemical modification of proteins. Reductive alkylation is the chemical reaction between amino groups and aldehyde groups, and produces alkylated amino groups through forming Schiff bases and their reduction (7). Using ^{13}C-enriched formaldehyde in this reaction, the amino groups are alkylated by up to two ^{13}C-methyl groups (8) (Figure 1.2).

This labeling scheme has several advantages. (i) The reaction proceeds under the mild condition for proteins, neutral pH and 4 °C, without significant side reaction. (ii) The pK_a value of amino groups changes only 0.5-1 unit upon the methylation, thus methylated amino groups are protonated and maintain positive charge at neutral pH. (iii) The methylation does not induce a severe change in global fold and function of the modified protein. Furthermore, the advantage in NMR sensitivity is expected because methyl groups generally give strong and sharp signal due to the rapid rotations around three-fold symmetry axes and showing

favorable relaxation properties. In addition, the methyl groups attached to lysine side-chains are expected to be useful for interaction studies because most of lysine side-chains seem to be exposed to the solvent.

By utilizing these advantages, lysine ^{13}C-methylation has been applied to probe molecular interactions. For recent example, ligand binding events to a G protein-coupled receptor were probed by the NMR analysis using lysine ^{13}C-methylation (9). While a G protein-coupled receptor is biologically important in signal transduction and then an important target of drug discovery, conventional NMR techniques are not enough to analyze. This is because such a protein is difficult to be produced and isotope-labeled using *E. coli* system. Therefore, the isotope labeling by lysine ^{13}C-methylation has potential to study such a difficult target to be studied.

1.3. Chemical Shift Perturbation

One of the advantages in protein NMR analysis is probing molecular interactions with relatively weak binding affinity, μM to mM dissociation constant (K_d). Chemical shift perturbation is the most frequently employed experiment to probe interactions (10). It simply analyzes the chemical shift changes and their transitions upon the binding of ligands/proteins to isotope-labeled proteins (Figure 1.3a). In general, ^{1}H-^{15}N HSQC spectra of ^{15}N-labeled proteins are measured, and the chemical shifts of backbone amide groups are recorded as fingerprint. The titration of the ligands/proteins into the ^{15}N-labeled protein causes the chemical shift changes of the atoms surrounding the binding surface when specific interaction exists (Figure 1.3b). The continuous chemical shift transition from free to bound state enables to assign the resonance of bound state and to estimate the residue involving interactions by comparing the amount of chemical shift changes. Moreover, the peak transition can be quantitatively analyzed to determine a K_d value (Figure 1.3c). Although such analysis is

limited to fast exchange condition, which indicates the exchange rate of complex formation/dissociation is faster enough than the chemical shift differences between the free and bound state, it is powerful analytical method in terms of obtaining information about both interaction sites and affinity. Therefore, the chemical shift perturbation is widely used.

The limit in sensitivity of the chemical shift perturbation experiments often causes problems. In the case of using ^{1}H-^{15}N HSQC spectra for backbone amide groups, sequential titration experiments require generally 50-200 μM protein concentration. This concentration range is usually higher than physiological concentration, thus nonspecific interactions and protein aggregation are induced in some cases. Moreover, large protein complex formation increases line widths and the sensitivity is reduced. Therefore, highly sensitive NMR probes is required for interaction studies.

1.4. Aim of This Study

Although there are several advantages in protein NMR analyses, lysine ^{13}C-methylation was mainly employed in the late 1970s to the early 1990s, and its utilities has not been proved enough, especially in analyzing protein-protein interactions. Therefore, this study focused on the utilization of ^{13}C-methylation of lysine residues for protein-protein interactions.

Protein-protein interactions play a key role to express cellular functions through enzymatic reactions, signal transductions and so on. The determination of the protein-protein interaction sites at atomic resolution is an important issue to understand biological processes and regulate protein functions, and for future drug discovery. NMR spectroscopy is a unique method to determine the protein-protein interaction sites at atomic resolution under physiological condition (11).

Lysine ^{13}C-methylation has been applied to the NMR analyses of the interactions between proteins and metals (12-16), small ligands (9,16-19), nucleic acids (20), glycans (21)

and peptides (12,16). For protein-protein interaction, only one report is available where the interactions between cytochrome *c* and cytochrome b_5 / cytochrome *c* peroxidase are studied (22). In these studies, the assignments of methylated-lysine methyl groups are given by pK_a values (13,17,18,20) and paramagnetic shifts (14,15,22), but these assignments are tentative and not completed. On the other hand, the assignments given by mutants are reliable (9,12,19,22), and this method is applicable to the complete assignments of the methylated-lysine methyl groups of methylated-calmodulin (12,19). Since the complete assignment is not available except for calmodulin, the utility of the lysine ^{13}C-methylation NMR method to monitor the protein-protein interaction is unclear.

In this study, the resonances of all methyl groups of the methylated-lysine residues were assigned for methylated-ubiquitin, and the chemical shift perturbations upon the binding of three interacting proteins were analyzed to determine the protein-protein interaction sites and the binding affinity. As the ubiquitin interacting proteins, YUH1, Dsk2 and p62 were selected. YUH1 is a yeast ubiquitin C-terminal hydrolase, and yeast Dsk2 and mouse p62 are the ubiquitin binding proteins containing the ubiquitin-associated (UBA) domain (23,24).

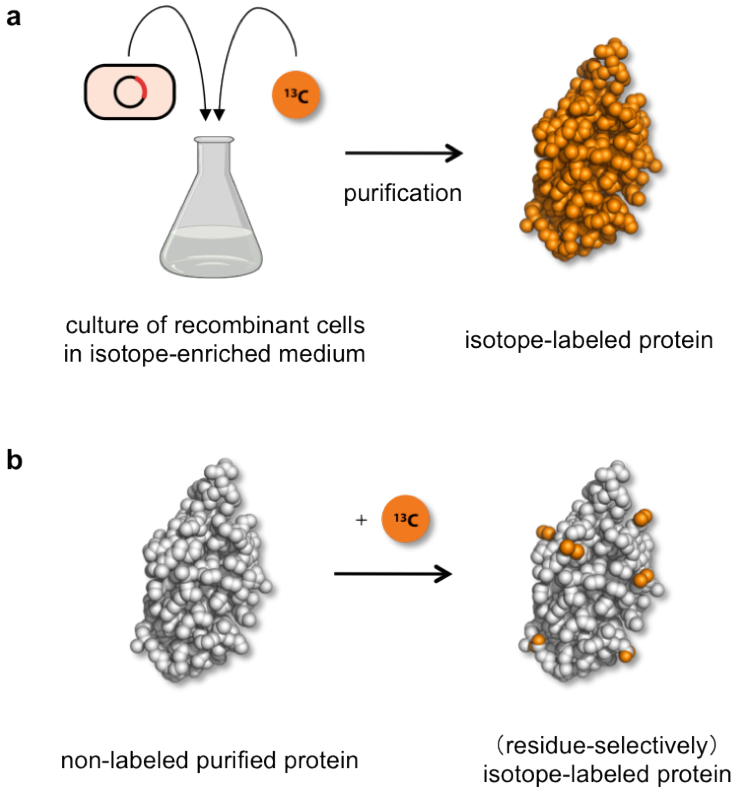

Figure 1.1. Schematic representation of the isotope labeling of proteins by (a) recombinant expression and (b) chemical modification.

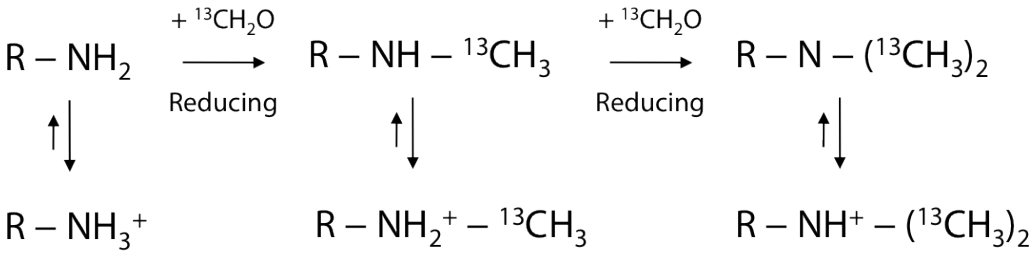

Figure 1.2. Reaction scheme of the ^{13}C-methylation of the amino group. One or two ^{13}C-methyl groups are conjugated to the amino group in the presence of ^{13}C-labeled formaldehyde in reduced conditions.

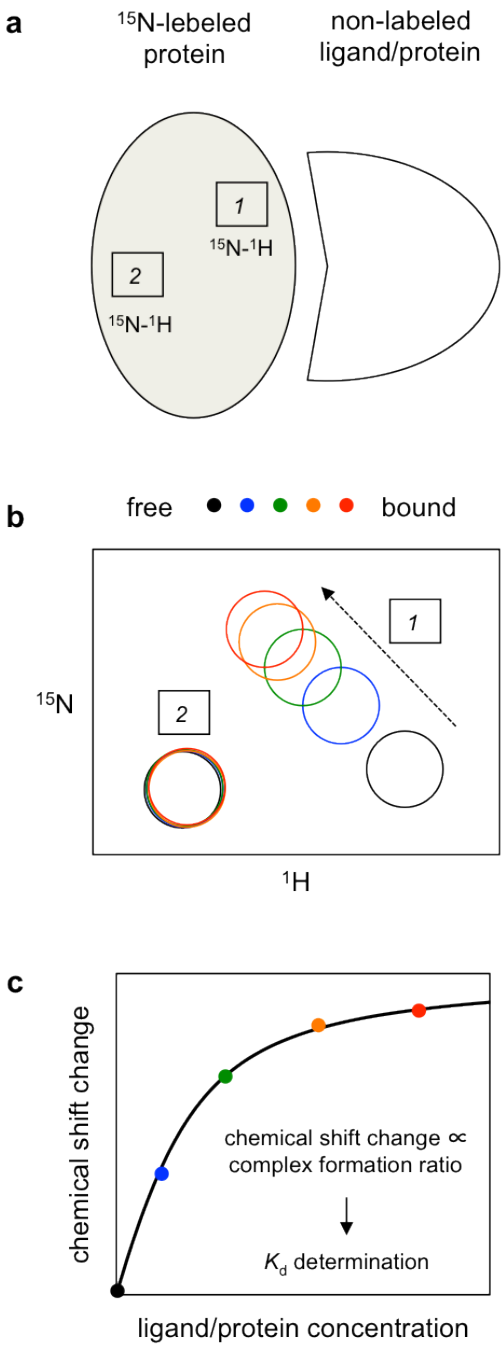

Figure 1.3. Schematic representation of chemical shift perturbation. (a) The interaction between ^{15}N-labeled protein and non-labeled ligand/protein. *1* and *2* represent the ^{15}N-^{1}H moieties close to and far from the binding interface, respectively. (b) Chemical shift changes from free (black) to bound (red) state shown in the two-dimensional NMR spectrum. (c) Titration curve of the chemical shift changes fitted for the determination of the K_d value.

2. Materials & Methods

2.1. Protein Expression and Purification

Recombinant *human* ubiquitin with a glutathione S-transferase (GST)-tag followed by a human rhinovirus 3C (HRV3C) cleavage sequence, LEVLFQGP, at the N-terminus was overexpressed in *E. coli* Rosetta(DE3). Uniformly ^{15}N-labeled ubiquitin was purified from *E. coli* cells cultured in M9 minimal media containing $^{15}NH_4Cl$. The cell culture was incubated at 37 °C until optical density at 600 nm (OD_{600}) 0.6–0.8, then protein expression was induced by adding isopropyl-b-D-thiogalactopyranoside (IPTG) to a final concentration of 0.5 mM, and incubation was continued at 37 °C for 6 h. After centrifugation of the culture, the pellet was frozen and stored at -80 °C. The frozen cells were thawed and lysed by sonication suspended in 50 mM tris(hydroxymethyl)aminomethane (Tris)-HCl (pH 8.0), 300 mM NaCl, 2 mM dithiothreitol (DTT), 0.5 mM ethylenediaminetetraacetic acid (EDTA) and 1 mM Pefabloc SC (Roche Diagnostics). The lysate was centrifuged at 35,000 rpm for 30 min at 4 °C using Type 45 Ti rotor (Beckman Coulter). The supernatant was loaded onto a 5 ml of Glutathione Sepharose 4B resin (GE Healthcare) and eluted with 50 mM Tris-HCl (pH 8.0) 300 mM NaCl and 30 mM reduced glutathione. Then HRV3C protease was added to cleave the GST-tag and incubated at 4 °C overnight. The solution was applied to a HiLoad 26/60 Superdex 75 pg (GE Healthcare). Protein concentration was determined by ultraviolet-visible (UV-Vis) absorption (ε_{280} = 1490 M^{-1} cm^{-1}). Lysine mutants (K6R, K11R, K27R, K29R, K33R, K48R and K63R) of ubiquitin were expressed and purified in the same way.

Recombinant *yeast* YUH1 with a C-terminal hexahistidine-tag was expressed in *E. coli* Rosetta(DE3) grown in LB medium. Cells were grown at 37 °C to OD_{600} 0.6, then protein expression was induced by IPTG at a final concentration of 0.5 mM for 4 h at 37 °C. The cultured cells were lysed by sonication and centrifuged. The supernatant was loaded onto the

affinity column with Ni-NTA Agarose (QIAGEN). The eluate was applied to the gel filtration column with HiLoad 26/60 Superdex 200 pg (GE Healthcare). Protein concentration was determined by UV-Vis absorption (ε_{280} = 28420 M^{-1} cm^{-1}).

Recombinant UBA domain of *yeast* Dsk2 ($Dsk2_{UBA}$) was prepare as reported (25). Briefly, the supernatant was loaded onto the affinity column. The protein was eluted, and thrombin protease was added to remove GST-tag. Then it was loaded onto the affinity column with Benzamidine Sepharose 6B (GE Healthcare) to remove the protease, and the eluate was applied to the gel filtration column with HiLoad 26/60 Superdex 75 pg (GE Healthcare). Recombinant UBA domain of *mouse* p62 ($p62_{UBA}$) was produced as previously described (26). Concentration of both $Dsk2_{UBA}$ and $p62_{UBA}$ was determined by UV-Vis absorption (ε_{280} = 1490 M^{-1} cm^{-1}).

Recombinant *human* 12 kDa FK506-binding protein (FKBP12) with a GST-tag followed by a sequence including HRV3C cleavage site, LEVLFQGPHM, at the N-terminus was overexpressed in *E. coli* Rosetta(DE3). Uniformly ^{15}N-labeled FKBP12 were purified from *E. coli* cells cultured in M9 minimal media containing $^{15}NH_4Cl$. The cell culture was incubated at 37 °C until OD_{600} 0.6–0.8, then protein expression was induced by adding IPTG to a final concentration of 0.5 mM, and incubation was continued at 37 °C for 6 h. After centrifugation of the culture, the pellet was frozen and stored at -80 °C. The frozen cells were thawed and lysed by sonication suspended in 50 mM Tris-HCl (pH 8.0), 300 mM NaCl, 2 mM DTT, 0.5 mM EDTA and 1 mM Pefabloc SC (Roche Diagnostics). The lysate was centrifuged at 35,000 rpm for 30 min at 4 °C using Type 45 Ti rotor (Beckman Coulter). The supernatant was loaded onto a 5 ml of Glutathione Sepharose 4B resin (GE Healthcare) and eluted with 50 mM Tris-HCl (pH 8.0), 300 mM NaCl and 30 mM reduced glutathione. Then HRV3C protease was added to cleave the GST-tag and incubated at 4 °C overnight. The solution was applied to a HiLoad 26/60 Superdex 75 pg (GE Healthcare). Protein

concentration was determined by UV-Vis absorption (ε_{280} = 9970 M^{-1} cm^{-1}). Lysine mutants of FKBP12 (K17R, K34R, K35R, K44R, K47R, K52R, K73R and K105R) were expressed and purified in the same way.

Recombinant *E. Coli* thioredoxin with an additional sequence including His-tag and Factor Xa cleavage site, MNHKVHHHHHHIEGRHM, at the N-terminus was overexpressed in *E. coli* Rosetta(DE3). Uniformly ^{15}N-labeled ubiquitin was purified from *E. coli* cells cultured in M9 minimal media containing $^{15}NH_4Cl$. The cell culture was incubated at 37 °C until OD_{600} 0.6–0.8, then protein expression was induced by adding IPTG to a final concentration of 0.5 mM, and incubation was continued at 15 °C overnight. After centrifugation of the culture, the pellet was frozen and stored at -80 °C. The frozen cells were thawed and lysed by sonication suspended in 50 mM Tris-HCl (pH 8.0), 300 mM NaCl, 20 mM imidazole, 2 mM DTT, 0.5 mM EDTA and 1 mM Pefabloc SC (Roche Diagnostics). The lysate was centrifuged at 35,000 rpm for 30 min at 4 °C using Type 45 Ti rotor (Beckman Coulter). The supernatant was loaded onto a 10 ml of Ni-NTA resin (QIAGEN) and eluted with 20, 50, 100 and 250 mM imidazole in 50 mM Tris-HCl (pH 8.0) and 300 mM NaCl. The eluted fractions containing thioredoxin were concentrated and applied to a HiLoad 26/60 Superdex 75 pg (GE Healthcare) equilibrated with 50 mM Tris-HCl (pH 8.0) and 100 mM NaCl. Then Factor Xa protease (Novagen) was added to cleave the His-tag with 5 mM $CaCl_2$ and incubated at 20 °C for 16 h. The solution was applied to a HiLoad 26/60 Superdex 75 pg (GE Healthcare). Protein concentration was determined by UV absorption (ε_{280} = 14105 M^{-1} cm^{-1}). Lysine mutants of thioredoxin (K19R, K34R, K35R, K45R, K48R, K53R, K74R and K106R) were expressed and purified in the same way without removal of the N-terminal additional sequence.

2.2. ^{13}C-methylation of Lysine Residues

The amino groups of ubiquitin, FKBP12 or thioredoxin were ^{13}C-methylated by reductive methylation technique using a protocol based on a previously published method (27). In general, 0.5 ml of 0.1 mM protein solution was prepared in 30 mM sodium phosphate (pH 6.8). 10 μl of freshly prepared 1 M dimethylamine borane (DMAB) (Wako Pure Chemical Industries) in water was added to the solution followed by the addition of 12.5, 14.1 or 18.8 μl of stock solution (~ 6.4 M) of ^{13}C-formaldehyde (Cambridge Isotope Laboratories) in the case of ubiquitin, FKBP12 and thioredoxin, respectively. The amount of formaldehyde is 100-fold compared to the amino groups in proteins. The mixture was incubated at 4 °C for 2 h. This step was repeated once more. Then 5 μl of 1 M DMAB was added and incubated at 4 °C overnight. Finally it was dialyzed to remove the excess reagents and exchange the buffer for an NMR measurement. The number of modified residues was evaluated by matrix assisted laser desorption/ionization-mass spectrometry (MALDI-MS) using sinapic acid as matrix.

Ubiquitin with the N-terminal GST-tag was methylated for the assignment of the N-terminal methyl groups of ubiquitin. The reaction protocol was the same except that the added volume of ^{13}C-labeled formaldehyde was totally 46.8 μl (2 times of 23.4 μl). HRV3C protease was added to the reactant to cleave the GST-tag. Then it was applied to the gel filtration column with HiLoad 26/60 Superdex 75 pg (GE Healthcare).

2.3. NMR Measurements

NMR samples of ^{13}C-methylated proteins were prepared at about 0.1 mM concentration of 260 μl solution in 30 mM sodium phosphate (pH 6.8) with 14 μl of D_2O as lock solvent (final ~ 5% D_2O). For the experiments with low protein concentrations, samples were prepared in 99.96% D_2O containing 10 mM sodium phosphate (pH 6.8). The mixed 274 μl

solution was filled in 5 mm microtubes (Shigemi) followed by degassing. NMR measurements were performed at 303 K on on 500, 800 and 950 MHz NMR spectrometers equipped with $^{1}H/^{13}C/^{15}N$ cryogenic probes, and on 400 and 500 MHz machines with $^{1}H/X$ and $^{1}H/^{13}C/^{15}N$ normal probes, respectively (Bruker Biospin).

Two-dimensional ^{1}H-^{13}C correlation spectra were acquired using a HSQC pulse sequence with gradient enhanced sensitivity improvement (28). The ^{13}C t_1 increments were 64–128 points for 10–20 ppm spectral width centered at 45.7 ppm. The scan number was set to 8 or 16 for each FID, and the total experimental time was within 1 h unless otherwise noted. For the titration experiments, the 500 MHz NMR was used. For low concentration samples, the 950 MHz NMR with cryogenic probe was used with the following parameters. ^{13}C t_1 increments were set to 32 points and extended to 64 points by linear prediction for 10.5 ppm spectral width, which corresponds to 2500 Hz for the 950 MHz NMR spectrometer. The scan numbers were set to 256 and 1024 for each FID for the free and YUH1 bound forms, and the total experimental times were 2 h 35 min and 10 h 20 min, respectively.

Two-dimensional ^{1}H-^{15}N correlation spectra for ubiquitin and methylated ubiquitin were acquired using FHSQC pulse sequence with WATERGATE (29). Backbone sequential assignments of ubiquitin and methylated ubiquitin were achieved using three-dimensional HNCA, HN(CO)CA, HN(CA)CB, HN(COCA)CB spectra (2,30). For YUH1 bound form, the assignments were achieved by tracing the titration shifts with the help of reported assignments (31). For the other bound forms, the assignments were achieved by only tracing the titration shifts.

The assignments of methylated-lysine methyl groups of methylated ubiquitin were performed using mutants (K6R, K11R, K27R, K29R, K33R, K48R and K63R). For the bound form, the assignments were performed by tracing peak shifts through the titration. For K11, the methyl groups showed untraceable changes upon YUH1 binding, thus the assignment was

performed using the K11R mutant.

The acquired data were processed and analyzed by NMRPipe (32) and Sparky (33), respectively. ^{1}H chemical shifts were referenced to the resonance frequency of 2,2-dimethyl-2-silapentane-5-sulfonic acid (DSS), and heteronuclear ^{13}C or ^{15}N chemical shifts were indirectly referenced to DSS using the ^{1}H/^{13}C or ^{1}H/^{15}N gyro magnetic ratio (34). The weighed averages of ^{1}H and ^{15}N chemical shift differences ($\Delta\delta_{H+N}$) were calculated by the equation $\Delta\delta_{H+N} = (\Delta\delta_{H}^{2} + (\Delta\delta_{N}/5)^{2})^{1/2}$, where $\Delta\delta_{H}$ and $\Delta\delta_{N}$ represent the differences in ^{1}H and ^{15}N chemical shifts (ppm), respectively.

2.4. NMR Titration Experiments

For the titration experiment with YUH1, the initial concentration of methylated ubiquitin was set to 0.05 mM, and 0.74 mM YUH1 was added to methylated ubiquitin with molar ratios of 0.20, 0.40, 0.80, 1.2, 2.0 and 4.0. For Dsk2$_{UBA}$, the initial concentration of methylated ubiquitin was set to 0.10 mM, and 0.93 mM Dsk2$_{UBA}$ was added to methylated ubiquitin with molar ratios of 0.18, 0.45, 0.88, 1.3, 2.2 and 4.0. For p62$_{UBA}$, the initial concentration of methylated ubiquitin was set to 0.10 mM, and 1.38 mM p62$_{UBA}$ was added to methylated ubiquitin with molar ratios of 0.46, 0.92, 1.8, 3.5 and 5.5.

K_d values of the 1:1 binding mode were calculated using the non-linear least square method by fitting of the K_d and also $\Delta\delta_{max}$ to the equation as

$$\Delta\delta_{obs} = \Delta\delta_{max}\frac{([P]_t + [L]_t + K_d) - \sqrt{([P]_t + [L]_t + K_d)^2 - 4[P]_t[L]_t}}{2[P]_t}$$

where $\Delta\delta_{obs}$ is the change in the observed shift from the free state, $\Delta\delta_{max}$ is the maximum shift change on saturation, $[P]_t$ is the total concentration of protein and $[L]_t$ is the total concentration of ligand.

The peaks showing titration shifts larger than the half of line width (~ 3 Hz) were used

in the calculation. Error for the K_d value was estimated by a Monte Carlo procedure. Experimental peak-position and the spectral digital resolution were assumed to be the means and variances of a Gaussian distribution, respectively. From each such distribution, 50 synthetic peak-position data sets were created. Calculation of the K_d value was performed for each of the 50 synthetic peak-position data sets. The standard deviation of the resulting ensemble of the K_d value was taken as the estimated error.

2.5. Isothermal Titration Calorimetry (ITC) Experiments

Before the ITC experiments, purified samples were dialyzed against 30 mM sodium phosphate (pH 6.8) and 100 mM NaCl. This dialysis buffer was used to measure heats of dilution. ITC experiments were performed at 298 K on Omega Micro Calorimeter (Microcal Inc.). 0.62 mM YUH1 was titrated 28 times every 5 minutes by 10 μl into 49 μM ubiquitin or 54 μM methylated ubiquitin. The experimental data were analyzed by the Origin-ITC software package (OriginLab). Heats of dilution were subtracted from the raw data before analysis.

2.6. Salt Bridge Analysis in Crystal Structures

N…O distances were calculated as distances between lysine Nζ atoms and centroids of most proximate aspartate Oδ1/Oδ2 or glutamate Oε1/Oε2 atoms in the coordinates of crystal structures for ubiquitin, FKBP12 and thioredoxin (Figure 2.1). Salt bridges are defined as N…O distances ≤ 4 Å (35,36). There are some crystal structures of ubiquitin, FKBP12 and thioredoxin submitted in PDB. For ubiquitin, 2 structures, 1UBQ and 1UBI are almost identical backbone structure, root-mean-square deviation (RMSD) is 0.09 Å, and N…O distance, then one of them, 1UBQ, are chosen as the representative. For FKBP12 and

thioredoxin, there are 4 structures (8 chains) and 2 structures (4 chains), respectively. These are similar but significant differences are found on backbone structure and N…O distance. Therefore the mean structure of them was calculated, and the structure with smallest RMSD to the mean was chosen as the representatives, which are 1D7J (chain B) and 2TRX (chain A) for FKBP12 and thioredoxin, respectively.

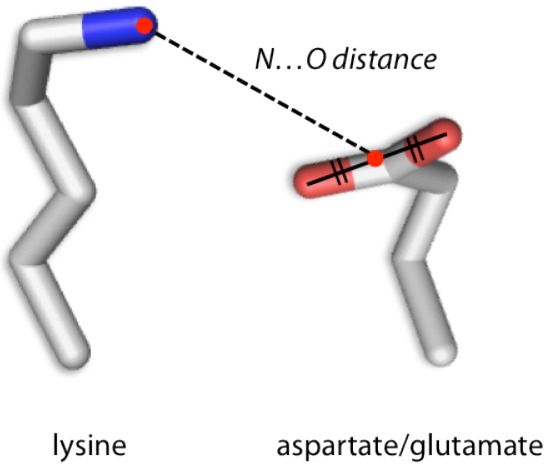

Figure 2.1. Schematic representation of N…O distance calculation. Atoms are shown by stick representation and colored as follows; carbon (gray), nitrogen (blue) and oxygen (red).

3. Results

3.1. NMR Spectra of Methylated-Ubiquitin

All amino groups, the lysine side-chain and the N-terminus, are potential chemical-methylation sites of protein. Ubiquitin possessing eight amino groups, seven lysine side-chains and one N-terminus was subjected to the chemical-methylation using excess ^{13}C-formaldehyde (200-fold of the reactive site). After the chemical-methylation, the molecular mass increased by 239.9 evaluated from MALDI-MS spectra, and it was identical to the calculated value 240.3 assuming two hydrogen atoms were replaced with $^{13}CH_3$ groups (^{13}C di-methylation) at all eight amino groups, within the error range. In the ^{1}H-^{13}C HSQC spectrum of the methylated ubiquitin (Figure 3.1a), all methyl peaks of methylated lysine appeared around 45 ppm in the ^{13}C dimension, representing all amino groups are di-methylated, since methyl signals of mono-methylated lysine appear around 35 ppm in the ^{13}C dimension (17). When less ^{13}C-formaldehyde (10-fold of the reactive site) was used for the chemical-methylation, the reaction was not completed and the methyl peaks appeared around both 35 and 45 ppm in the ^{13}C dimension (Figure 3.1b). These data indicated that, under the experimental condition using 200-fold ^{13}C-formaldehyde, all amino groups of lysine residues and N-terminus of ubiquitin were fully di-methylated. It is noted that the fully di-methylated sample makes the required spectral width narrower in the ^{13}C dimension and the resulted experimental time shorter.

The resonance assignment of the methylated-lysine methyl groups of the fully di-methylated ubiquitin, hereinafter called as *methylated ubiquitin*, was performed by the point mutation of each lysine to arginine, and the digesting the N-terminal GST-tag of the methylated GST-ubiquitin fusion protein (Figure 3.2). From the spectra of the mutants and the digested product, it was evident that peaks had disappeared without obvious shifts of other

peaks. Under the experimental condition of 303 K and pH 6.8, the line shape was different to each other especially in the ^{13}C dimension. After changing the magnetic field from 400 to 950 MHz, it was found that K27 was in slow exchange on the NMR time scale, K11 was in slow to intermediate exchange, K29 was in intermediate to fast exchange, and all others were in fast exchange (Figure 3.2). An apparent correlation was observed between these line shape differences and the reported generalized order parameters, S^2, of the lysine amino groups of ubiquitin (37). That is, K27 showed the largest S^2 value (0.71) on the lysine amino group and slow exchange on the ^{13}C methylated-lysine methyl groups, K11 and K29 showed the larger S^2 values (0.42 and 0.38, respectively) and intermediate exchange, and the others showed the smaller S^2 values (less than 0.3) and fast exchange.

It has been discussed that slowing the exchange rate between two methyl groups of the di-methylated lysine is correlated to making a salt bridge (9,14,38). Indeed, for K11 and K27, the distances between the lysine Nζ and the centroids of carboxyl oxygens were within the salt-bridge distance (≤ 4 Å) (39) in the crystal structure of non-methylated ubiquitin (40). For K29, the lysine side chain did not form the salt bridge, but the distance between the lysine N^{ζ} and backbone carbonyl oxygen was within the hydrogen-bond distance (≤ 3.5 Å) (41), and the *J*-coupling between $^{15}N\zeta$ and carbonyl ^{13}C nuclei across the hydrogen bond were observed (42).

3.2. Ubiquitin-YUH1 Interaction

ITC experiments were performed to evaluate the effect of the methylation on the protein- protein interaction. Either of non-methylated ubiquitin and *methylated ubiquitin* was titrated into YUH1. The K_d values of YUH1 with non-methylated ubiquitin and *methylated ubiquitin* were determined to be 9.4 ± 2.6 and 5.7 ± 2.3 μM, respectively (Table 3.1). The K_d value of *methylated ubiquitin* was slightly smaller than the value of non-methylated ubiquitin.

However, the binding mode was considered to be quite similar, since the changes in enthalpy and entropy values of non-methylated ubiquitin and *methylated ubiquitin* upon the binding to YUH1 are in very good agreement each other. To confirm this assumption, the conventional ^{1}H and ^{15}N chemical shift perturbation experiments were performed for non-methylated ubiquitin and *methylated ubiquitin* using ^{1}H-^{15}N HSQC spectra. The chemical shift changes of the backbone amide groups were well correlated between non-methylated ubiquitin and *methylated ubiquitin* (Figure 3.3). These ITC and NMR data suggest that, in this system, the binding interface does not change by the methylation.

Using the lysine ^{13}C-methylation NMR, the chemical shift perturbation experiment is applied to monitor the interaction between *methylated ubiquitin* and YUH1. ^{1}H-^{13}C HSQC spectra of the ^{13}C methylated-lysine methyl groups were measured (Figure 3.4a), and ^{1}H chemical shift changes were used for further analyses. For split peaks, the averaged chemical shift value was used to show the chemical shift change. K6, K11, K27 and K48 showed the significant changes $\geq$ 0.01 ppm in ^{1}H chemical shift (Figure 3.4b). All amino groups of these residues were located on the binding interface between ubiquitin and YUH1 in crystal structure of the complex (Figure 3.4c) (43). The binding interface was judged by the intermolecular distance, within 6 Å (44). All ^{1}H chemical shift changes except for K11 were used for the K_d value determination. K11 was in slow to intermediate exchange and the titration curve was not obtained. Fitting 4 titration curves simultaneously, the K_d value was determined to be 5.6 ± 1.3 μM assuming 1:1 binding stoichiometry (Figure 3.4d), and consistent with the value 5.7 ± 2.3 μM determined by the ITC experiment.

3.3. Ubiquitin-Dsk2$_{UBA}$ Interaction

The chemical shift perturbation experiment is applied to monitor the interaction between *methylated ubiquitin* and Dsk2$_{UBA}$ using the lysine ^{13}C-methylation NMR (Figure

3.5a). K6, K11 and K48 showed the significant changes ≥ 0.01 ppm in ^{1}H chemical shift in ^{1}H-^{13}C HSQC (Figure 3.5b). The amino groups of K6, K11 and K48 were 3.1 ± 1.0 Å, 13.4 ± 0.5 Å and 5.8 ± 0.7 Å apart from the binding interface between ubiquitin and Dsk2$_{UBA}$ in NMR structure of the complex (25), respectively. Thus, the amino groups of K6 and K48 were located on the interface, but K11 was not (Figure 3.5c). The significant but much smaller shift changes of K11 may be due to the structural change induced by the ubiquitin-Dsk2$_{UBA}$ complex formation, in fact, the RMSD values between free ubiquitin and ubiquitin-Dsk2$_{UBA}$ complex were larger than 1 Å on the β1-β2 loop where K11 locates. Fitting 5 titration curves simultaneously, the K_d value was determined to be 2.9 ± 1.4 μM assuming 1:1 binding stoichiometry (Figure 3.5d). This value was comparable but significantly smaller than the previously reported value of 14.8 ± 5.3 μM determined by the surface plasmon resonance experiment for *yeast* ubiquitin (25). This difference of the K_d value may be explained by the difference of the experimental conditions such as buffer, salt concentration and pH, and potentially the presence of the methylation.

3.4. Ubiquitin-p62$_{UBA}$ Interaction

The chemical shift perturbation experiment is applied to monitor the interaction between *methylated ubiquitin* and p62$_{UBA}$ using the lysine ^{13}C-methylation NMR (Figure 3.6a). K6 and K48 showed the significant changes ≥ 0.01 ppm in ^{1}H chemical shift in ^{1}H-^{13}C HSQC (Figure 3.6b). As shown in Figure 4c, p62$_{UBA}$ monomer binds ubiquitin using same binding mode with other canonical UBA domains, and p62$_{UBA}$ dimer does not bind ubiquitin (26). In this modeled structure (Figure 4c), the amino groups of K6 and K48 were located on the binding interface between ubiquitin and p62$_{UBA}$. Since both p62$_{UBA}$ and Dsk2$_{UBA}$ belong to the canonical UBA domain family, the binding interface of the p62$_{UBA}$ complex is expected to be similar to that of the Dsk2$_{UBA}$ complex. For the Dsk2$_{UBA}$ complex, K6, K11 and K48

showed the significant changes ≥ 0.01 ppm, and K6 and K48 showed the largest and the second largest shifts, respectively (Figure 3.6c). This tendency was kept in the $p62_{UBA}$ complex except that the magnitude of the change was much smaller. For example, K11 of the $p62_{UBA}$ complex showed the third largest shifts consistent with the $Dsk2_{UBA}$ complex, but the magnitude was smaller than 0.01 ppm.

In an effort to determine the K_d value between *methylated ubiquitin* and $p62_{UBA}$ monomer, 3 titration curves were fitted simultaneously assuming 1:1 binding stoichiometry. However the titration curves did not fit well with 1:1 binding mode. It has been reported that the K_d value of $p62_{UBA}$ dimer formation is 3.5 μM (26) and the dimerization is much stronger than ubiquitin binding (26,45). Thus we assumed the presence of two equilibriums, K_d = [ubiquitin][$p62_{UBA}$] / [ubiquitin-$p62_{UBA}$] and K_d(dimer) = [$p62_{UBA}$]^2 / [$p62_{UBA}$-$p62_{UBA}$] = 3.5 μM, where [ubiquitin], [$p62_{UBA}$], [ubiquitin-$p62_{UBA}$] and [$p62_{UBA}$-$p62_{UBA}$] are the concentration of *methylated ubiquitin*, $p62_{UBA}$, the complex between *methylated ubiquitin* and $p62_{UBA}$ monomer, and $p62_{UBA}$ dimer, respectively. Since $p62_{UBA}$ dimer does not bind ubiquitin (26), two equilibriums are enough to describe the whole system. Thus, 3 titration curves were fitted simultaneously assuming these two equilibriums. The titration curves fitted very well, and the K_d value between *methylated ubiquitin* and $p62_{UBA}$ monomer was determined to be 24 ± 3 μM (Figure 3.6d). This value was comparable to the previously reported values of a few tens μM (26) and 40 ± 10 μM (45) determined by the NMR experiments. In this two-equilibrium system, the chemical shift perturbation using the lysine ^{13}C-methylation NMR gave the precise K_d value consisting with the reported values, despite the chemical shift changes were small and the K_d value was large.

Table 3.1. ITC parameters of non-methylated ubiquitin or *methylated ubiquitin* titration of YUH1[#]

	non-methylated	methylated
N	0.95 ± 0.06	1.02 ± 0.06
*K*d [μM]	9.4 ± 2.6	5.7 ± 2.3
Δ*H* [kJ mol^{-1}]	-16.9 ± 1.4	-16.8 ± 1.4
Δ*S* [J K^{-1} mol^{-1}]	39.7 ± 5.3	43.9 ± 5.8

[#]*N*, K_d, Δ*H* and Δ*S* are the stoichiometry, dissociation constant, enthalpy change and entropy change, respectively.

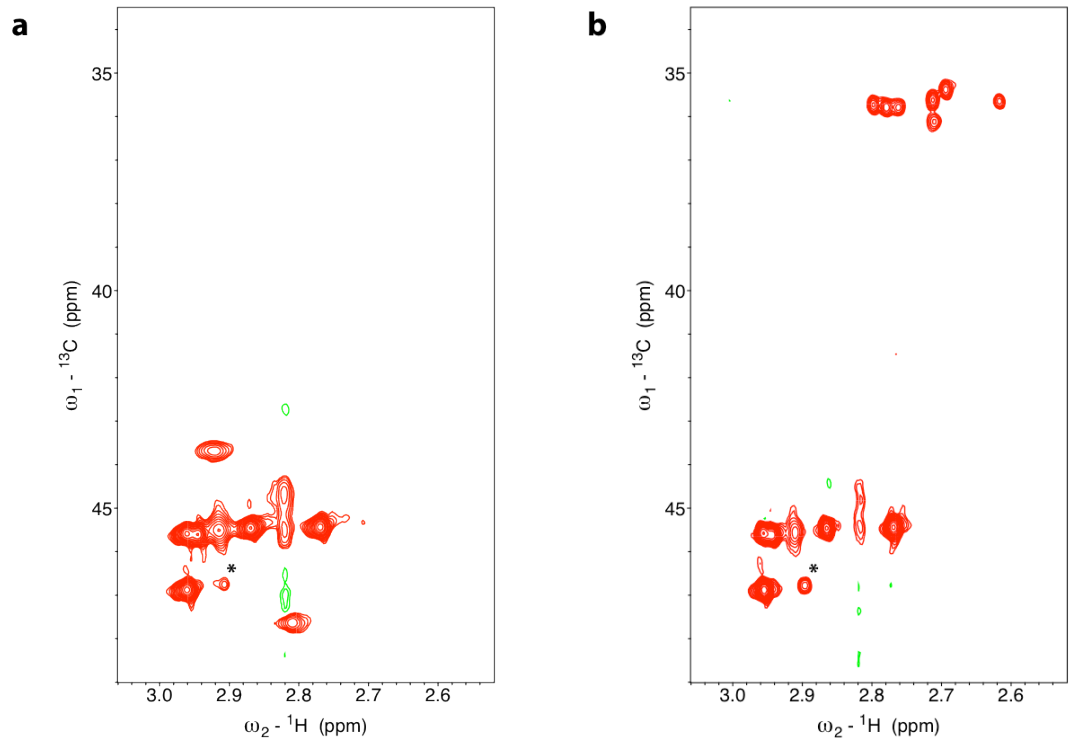

Figure 3.1. ^{1}H-^{13}C HSQC spectra of fully (a) or partially (b) di-methylated ubiquitin. Ubiquitin is methylated using 200-fold (a) or 10-fold (b) of ^{13}C-formaldehyde. Methyl signals of the mono-methylated and di-methylated lysine are observed around 35 and 45 ppm in the ^{13}C dimension, respectively. * indicates the minor peak from N-terminus.

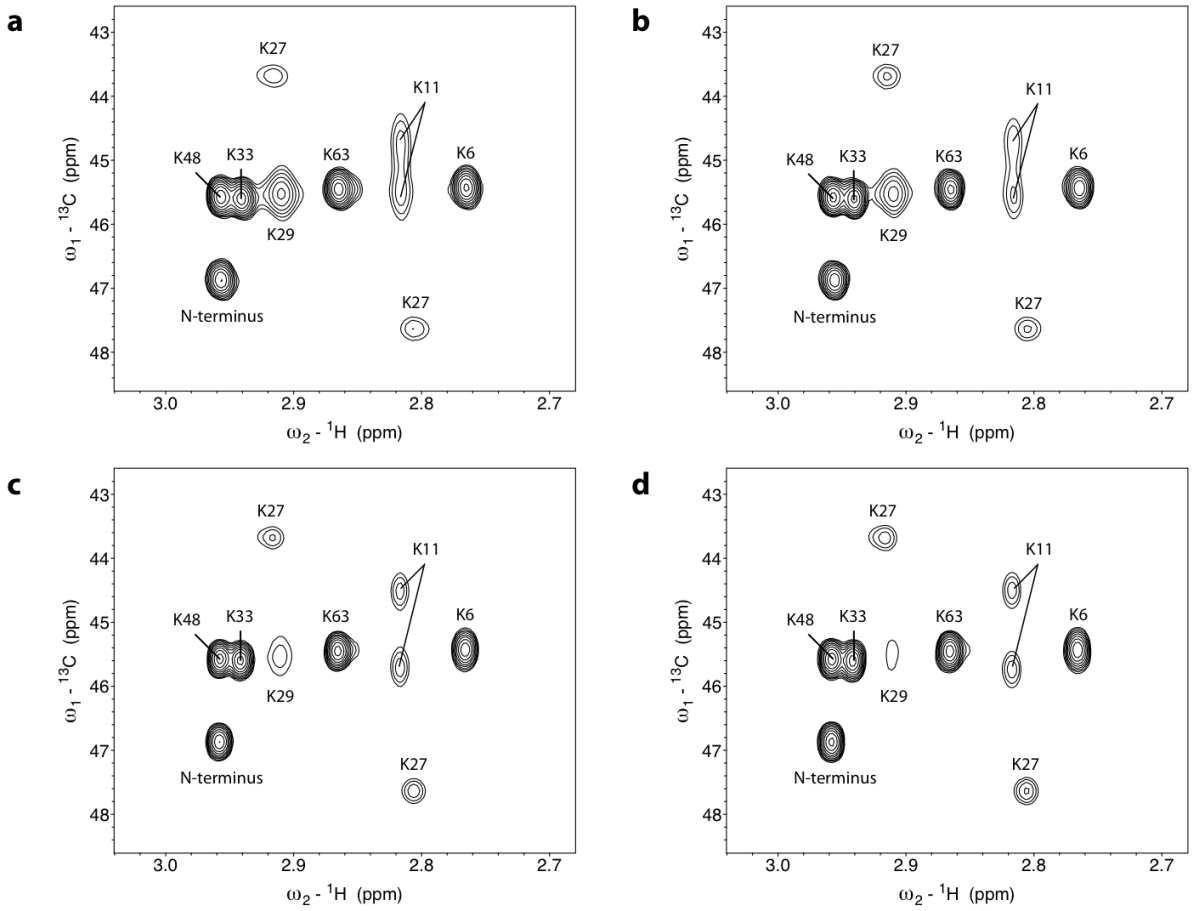

Figure 3.2. ^{1}H-^{13}C HSQC spectra of *methylated ubiquitin* and its resonance assignment. K11 and K27 give two peaks owing to slow exchange. The NMR spectra are acquired at (a) 400 MHz, (b) 500 MHz, (c) 800 MHz and (d) 950 MHz.

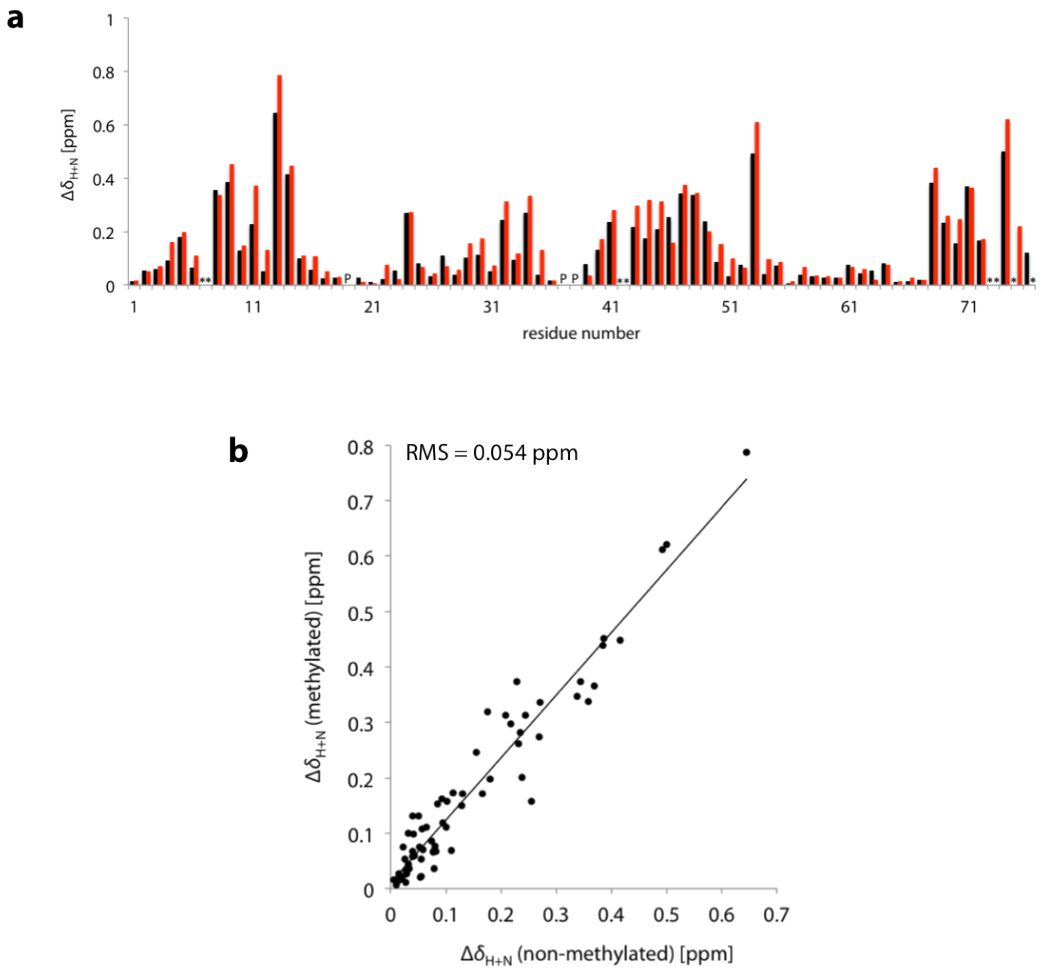

Figure 3.3. ^{1}H and ^{15}N chemical shift changes of non-methylated ubiquitin and *methylated ubiquitin* in the presence of YUH1. (a) The averaged ^{1}H and ^{15}N chemical shift changes of non-methylated ubiquitin (red) and *methylated ubiquitin* (black) in the presence of YUH1. * and the letter P indicates the unassigned and proline residues, respectively. (b) The correlation plots of the chemical shift changes of non-methylated ubiquitin and *methylated ubiquitin*. The best-fit line is given.

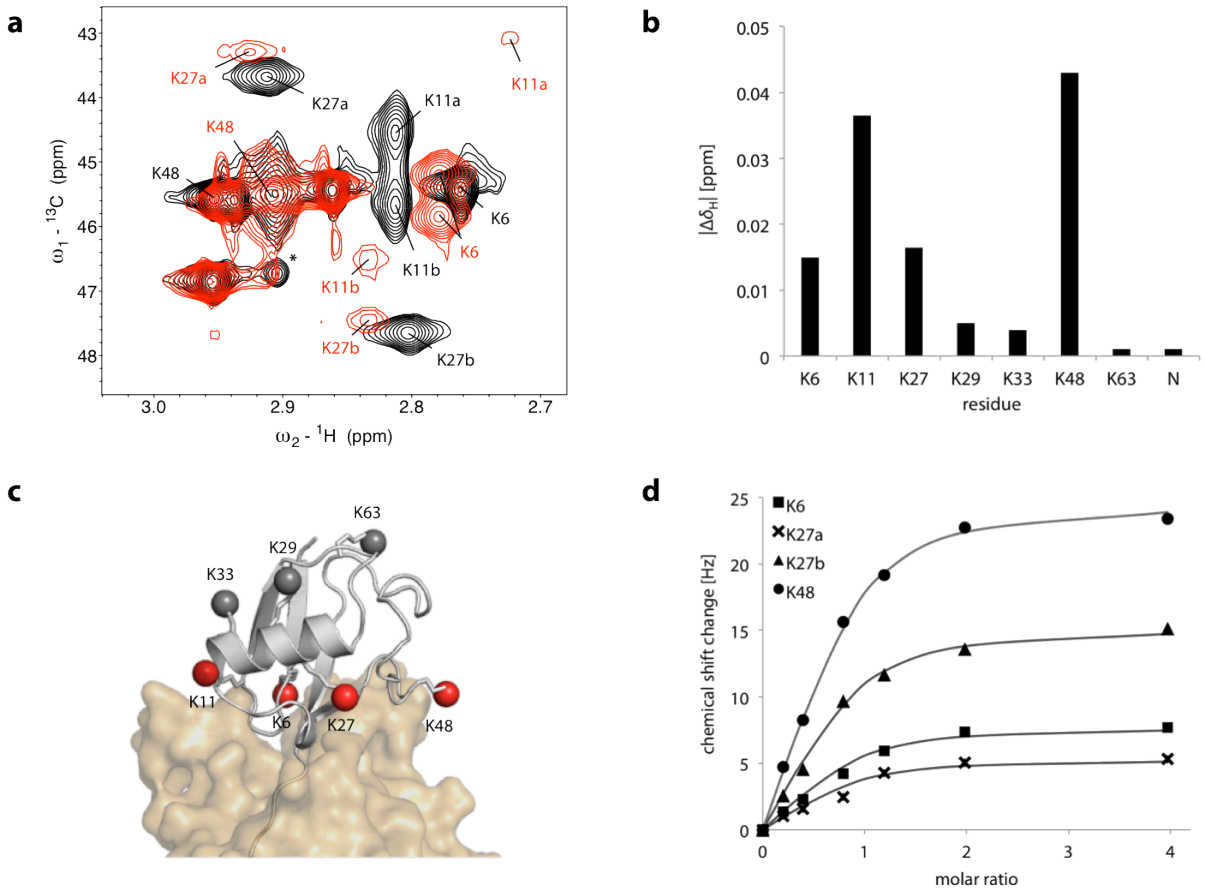

Figure 3.4. Titration experiments by lysine ^{13}C-methylation NMR. YUH1 is titrated to *methylated ubiquitin* and monitored by the methylated-lysine methyl groups. (a) The overlay of the ^{1}H-^{13}C HSQC spectra of *methylated-ubiquitin* (black) and *methylated-ubiquitin* with 4-fold YUH1 (red). * indicates the minor peak from N-terminus. (b) Absolute values of the ^{1}H chemical shift changes of *methylated ubiquitin* in the presence of YUH1. The changes of the split peaks are averaged. (c) Ubiquitin-YUH1 complex structure (PDB ID: 1CMX). Ubiquitin and YUH1 are shown by the ribbon and surface representation, respectively. Lysine Nζ atoms of ubiquitin are shown by spheres. Chemical shift changes larger and smaller than 0.01 ppm were colored by red and gray, respectively. (d) Titration curves for K6, K27a, K27b and K48 of *methylated-ubiquitin*. The K_d value of *methylated ubiquitin* and YUH1 was 5.6 ± 1.3 μM.

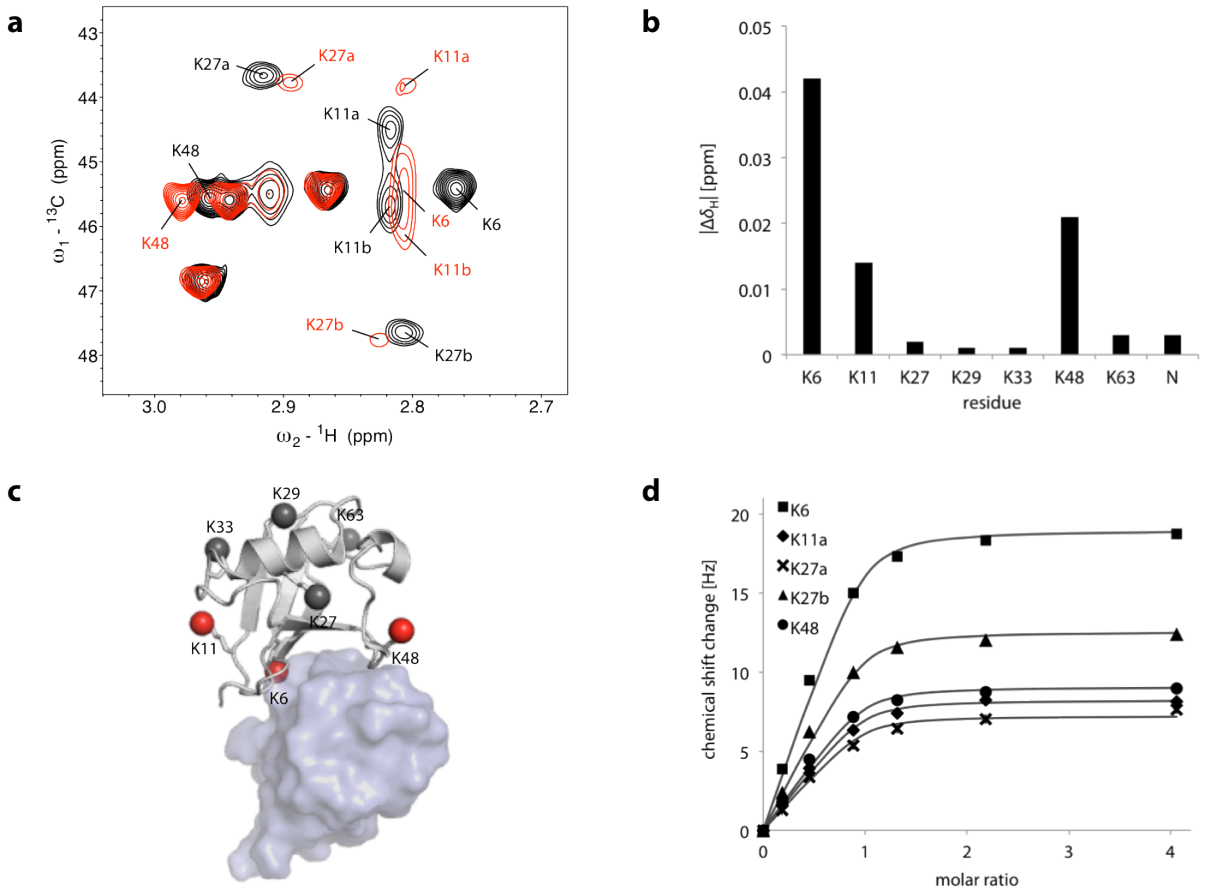

Figure 3.5. Titration experiments by lysine ^{13}C-methylation NMR. Dsk2$_{UBA}$ is titrated to *methylated ubiquitin* and monitored by the methylated-lysine methyl groups. (a) The overlay of the ^{1}H-^{13}C HSQC spectra of *methylated ubiquitin* (black) and *methylated ubiquitin* with 4-fold Dsk2$_{UBA}$ (red). * indicates the minor peak from N-terminus. (b) Absolute values of the ^{1}H chemical shift changes of *methylated ubiquitin* in the presence of Dsk2$_{UBA}$. The changes of the split peaks are averaged. (c) Ubiquitin-Dsk2$_{UBA}$ complex structure (PDB ID: 1WR1). Ubiquitin and Dsk2$_{UBA}$ are shown by the ribbon and surface representation, respectively. Lysine Nζ atoms of ubiquitin are shown by spheres. Chemical shift changes larger and smaller than 0.01 ppm were colored by red and gray, respectively. (d) Titration curves for K6, K11a, K27a, K27b and K48 of *methylated ubiquitin*. The K_d value of *methylated ubiquitin* and Dsk2$_{UBA}$ was 2.9 ± 1.4 μM.

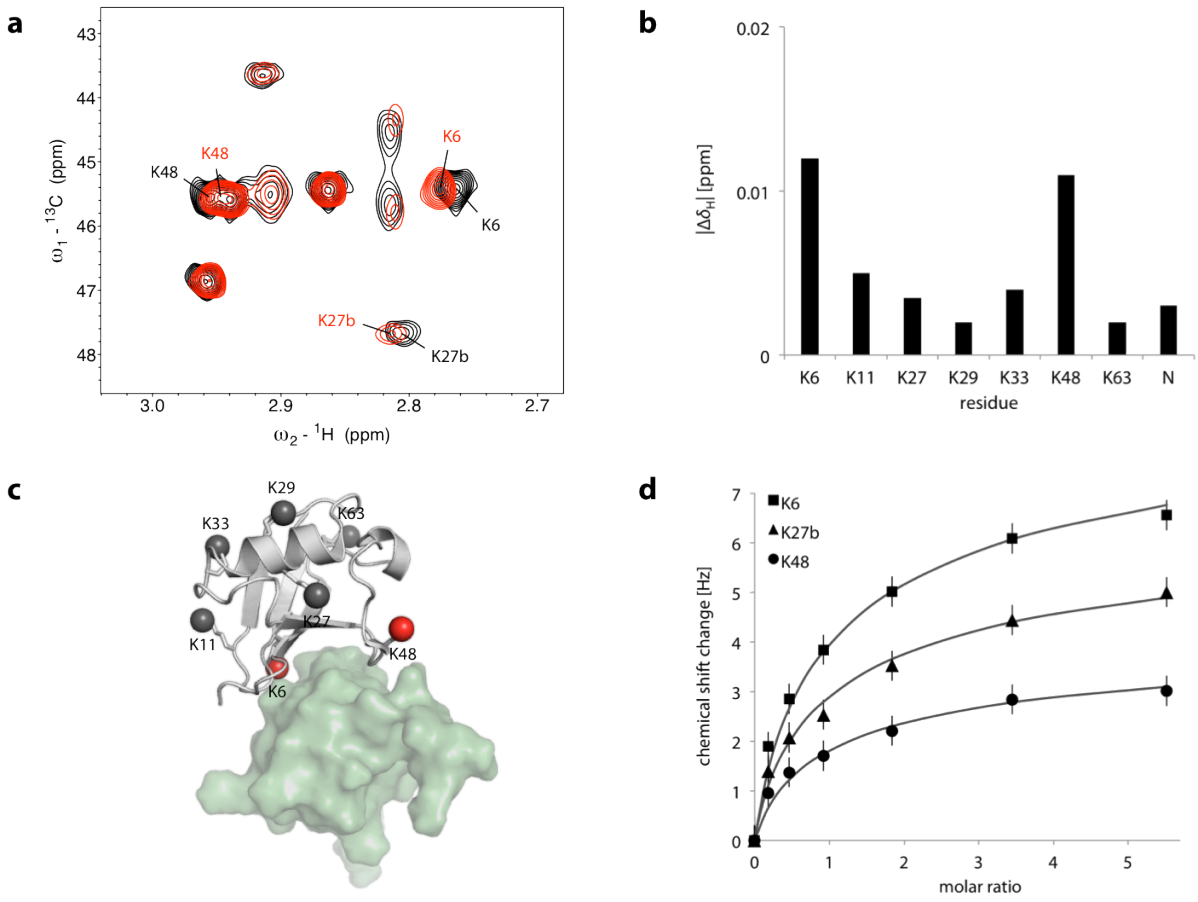

Figure 3.6. Titration experiments by lysine ^{13}C-methylation NMR. $p62_{UBA}$ is titrated to *methylated ubiquitin* and monitored by the methylated-lysine methyl groups. (a) The overlay of the ^{1}H-^{13}C HSQC spectra of *methylated ubiquitin* (black) and *methylated ubiquitin* with 5.5-fold $p62_{UBA}$ (red). * indicates the minor peak from N-terminus. (b) Absolute values of the ^{1}H chemical shift changes of *methylated-ubiquitin* in the presence of $p62_{UBA}$. The changes of the split peaks are averaged. (c) Modeled structure of ubiquitin-$p62_{UBA}$ complex based on the ubiquitin-$Dsk2_{UBA}$ complex structure (PDB ID: 1WR1) and ubiquitin bound form of $p62_{UBA}$ structure (PDB ID: 2RRU). Ubiquitin and $p62_{UBA}$ are shown by the ribbon and surface representation, respectively. Lysine Nζ atoms of ubiquitin are shown by spheres. Chemical shift changes larger and smaller than 0.01 ppm were colored by red and gray, respectively. (d) Titration curves for K6, K27b and K48 of *methylated ubiquitin*. The K_d value of *methylated ubiquitin* and $p62_{UBA}$ was 24 ± 3 μM.

4. Discussion

4.1. Side-Chain Interaction

In the lysine ^{13}C-methylation NMR, the protein-protein interaction is monitored by the chemical shift perturbation of the methyl signals using the ^{1}H-^{13}C HSQC spectra. The introduced methyl groups are located on the terminus of the long side-chain of lysine, apart from the backbone amide group by up to 7 Å. Therefore, the chemical shift perturbation pattern will be different somewhat between the side-chain methyl groups and the backbone amide groups. In an effort to estimate this difference, the chemical shift perturbation experiments of the backbone amide groups of the *methylated ubiquitin* were performed using the ^{1}H-^{15}N HSQC spectra for YUH1, Dsk2$_{UBA}$ and p62$_{UBA}$ (Figure 4.1), and compared with those of the side-chain methyl groups (Figure 4.2).

The chemical shift perturbation pattern was not different for many residues between the side-chain methyl groups and the backbone amide groups, however, some significantly large differences were found. Among them, K6 and K48 residues in Dsk2$_{UBA}$ binding showed the most significant differences (Figure 4.2b). The K6 methyl groups showed the largest change among all methyl groups, but the K6 amide group showed the small change. This agreed with that the side-chain amino group of K6 forms the hydrogen bond with the side-chain carbonyl group of Q338 of Dsk2$_{UBA}$, and the backbone amide group has no such specific interaction (Figure 4.2d and Table 4.2). Similar patterns were found in the changes of K6 and K27 in YUH1 binding, and K6 in p62$_{UBA}$ binding. As well, this agreed with that the side-chain amino groups of K6 and K27 are located on the interface in YUH1 binding, and the backbone amide group is not (Table 4.2). It is noted that the all lysine residues located on the binding interface show the significant chemical shift changes of the methyl groups ($\geq$ 0.01 ppm), but the half residues do not show the significant changes of the backbone amide groups ($\geq$ 0.2 ppm). That

is, for the half residues, the backbone N atoms are not located on the binding interface (Table 4.2). These data are consistent with the nature that the lysine side-chain amino group tends to locate on the binding interface, but the backbone amide group is apart from the side-chain up to 7 Å and fails to locate on the binding interface. Therefore, the methylated-lysine methyl groups are good probes to monitor the protein-protein interaction, that is, very sensitive to the side-chain interaction, which cannot be detected by the backbone amide groups.

4.2. NMR Sensitivity

In general, the methyl group NMR gives the strongest signals for the protein sample, and the selective labeling of methyl groups is widely used to study the large protein complexes (46). Thus, the sensitivity of lysine ^{13}C-methylation NMR is expected to be high independently of molecular weight and resonance frequency. To evaluate the sensitivity, the lysine ^{13}C-methylation NMR was applied to the 2 and 0.2 μM *methylated ubiquitin* samples to monitor the protein-protein interaction using 950 MHz NMR spectrometer with cryogenic probe (Figure 4.3). At 2 μM, all peaks of methylated-lysine methyl groups were observed. In the presence of YUH1, K29 signal was missing but all other peaks including the shifted peaks of K6, K11, K27 and K48 were detected. At 0.2 μM, all peaks of methylated-lysine methyl groups were observed, except for K29. In the presence of YUH1, all peaks were observed except for K11, K27 and K29. These missing residues are in slow to intermediate exchange (Figure 3.2), and their signal intensities were much weaker than the others even in the free state. In this sense, the resonance frequency affects the sensitivity through the line shape change due to the exchange process. These data suggest that the sensitivity of the lysine ^{13}C-methylation NMR is very high and applicable to the low concentration sample, at least sub-μM using the state-of-the-art NMR hardware, to monitor the protein-protein interaction.

4.3. Methylation Reactivity

The lysine ^{13}C-methylation NMR is applicable for a wide range of targets because the methylation reaction proceeds at neutral pH and 4 °C. The protein function is expected to be maintained because the methylated lysine keeps the similar pK_a value for the Nζ atom and protonated at neutral pH (17,47). The lysine methylation also improves the crystallization probability (27,48). In this report, the fully di-methylated ubiquitin is prepared by using 200-fold formaldehyde and mainly used. When the amount of the formaldehyde was decreased, the ratio of the di-methylated lysine was decreased drastically (Figure 4.4a). The reactivity was obviously different from one residue to another. For example, K6 and K27 were most and least reactive residues, respectively. When the 40-fold formaldehyde was used instead of 200-fold, most lysine residues were di-methylated but K27 were not. The reactivity depended on the solvent accessibility, and the positive correlation between them was observed (Figure 4.4b). The solvent accessibilities were calculated by GetArea (49) using the crystal structure (PDB ID: 1UBQ) and the radius of the water probe was set to 1.4 Å. The least reactive residue K27 showed the smallest solvent accessibility by far. The reactivity also depended on the reported apparent pK_a values (50), and the negative correlation between them was observed (Figure 4.4c). This relation is reasonable because the methylation reaction includes the de-protonation of the amino groups.

4.4. Structural Change by Methylation

In lysine ^{13}C-methylation NMR, ^{13}C-methyl groups are conjugated to all amino groups of the protein, which may cause the structural change of the methylated protein. In an effort to evaluate the structural change induced by the methylation, PDB database was surveyed. More than 100 crystal structures of the methylated proteins were found. For 16 proteins, both

non-methylated and methylated structures were found, and the RMSD values of backbone C_α atoms between non-methylated and methylated structures were calculated (Table 4.1). The averaged RMSD value was 0.5 ± 0.3 Å, and the maximum RMSD value was 1.05 Å. These numbers mean that no or little structural change is induced by the lysine methylation.

The structural change induced by the lysine methylation was further studied using NMR. ^{1}H-^{15}N HSQC spectra were measured for non-methylated ubiquitin and *methylated ubiquitin* (Figure 4.5a), and the significant changes were observed (Figure 4.6a). The significantly large changes ≥ 0.4 ppm were observed for the residues, E24, D39 and G53. These residues were mapped on the ubiquitin structure, and located spatially close to K27 (Figure 4.6b). K27 was the most buried residue, and its solvent accessibility was less than 10%. The methylation of the buried lysine may cause the detectable structural change. As described above, the reactivity of K27 was significantly lower than the others. When the amount of formaldehyde was reduced (10-fold of the reactive site), the observed chemical shift changes were suppressed in the ^{1}H-^{15}N HSQC spectra (Figure 4.5b). Under this reaction condition, all methyl peaks of di-methylated-lysine methyl groups except for K27 were observed in the ^{1}H-^{13}C HSQC spectrum. Therefore, using an appropriate amount of formaldehyde, the buried lysine residue can be excluded in the methylation reaction, and the structural change induced by the lysine methylation can be kept at a minimum.

4.5. Intramolecular Interaction

In chapter 3.1, the ^{1}H-^{13}C HSQC spectrum of *methylated ubiquitin* suggested that the line shape is related to the intramolecular interaction mode of the lysine side-chain. For the further investigation about the correlation between NMR spectral patterns and lysine side-chain interactions, ^{1}H-^{13}C HSQC spectra of other two proteins, FKBP12 and thioredoxin, in fully di-methylated form were obtained. Their resonance assignments were performed

(Figure 4.7).

Although all of the NMR signals of the methyl groups attached to lysine residues were observed, their splitting and line width were different. Of all 25 residues in three proteins, 11 residues were assigned to the singlet peaks with narrow line widths, 6 residues were singlet with broad line widths, especially in the ^{13}C dimension (line width is larger than 20 Hz), and 8 residues were "split" to doublet or multiplet. In order to investigate the relationship between these splitting patterns and lysine side-chain interaction modes such as "salt bridge" and "hydrogen bond with backbone", the splitting patterns were classified into "split", "broad" and "singlet", and the interaction modes were classified into "salt bridge", "hydrogen bond with backbone" and "no interaction" (Table 4.3). The table showed that 7 of 8 "split" residues, 3 of 6 "broad" residues and none of 11 "singlet" residues were assigned to "salt bridge". That is, the methyl groups in the methylated-lysine residues involved in salt bridge interactions showed slow to intermediate chemical exchanges. The "broad" residues were assigned to not only "salt bridge" but also "hydrogen bond with backbone".

The correlation between the chemical shift of the methyl groups and salt bridge formation of lysine residues was discovered. In Figure 4.8, the plot between the ^{1}H and ^{13}C chemical shifts was shown. The chemical shift values were averaged for the split peaks. The "salt bridge" residues represented as open circles showed upfield-shift in both ^{1}H and ^{13}C chemical shifts. On the other hand, the residues without "salt bridge" represented as filled circles showed no significant shifts. UBQ K6, TRX K52 and TRX K57 are spatially close (< 6 Å) to aromatic rings. The upfield shifts of these residues, which shows different trend compared to the "salt bridge" residues seem to be influenced by ring current effect.

In general, hydrogen bonding induces downfield-shift in ^{1}H chemical shifts. Thus the methyl groups might not be involved in hydrogen bonding and the carboxyl groups, spatially close to the methyl groups, might induce upfield-shift. The through-space upfield-shift

changes may be due to the electric field effect (51) of the negative charge in the carboxyl groups, and/or local magnetic anisotropy effect (52) of the C=O bonds in the carboxyl groups. The upfield-shift trends supposed that salt bridges to the methylated-lysine side-chains might not be stabilized by methyl-carboxyl hydrogen bonds, but by amino-carboxyl hydrogen bonds. But finally, it is noted that further investigation such as theoretical calculation study is needed for the confirmation of these hypotheses.

Table 4.1. Cα RMSD values between non-methylated and methylated proteins.

Uniprot ID	PDB ID (non-methylated)	PDB ID (methylated)	Cα RMSD[#] [Å]
P00698	1LYZ	132L	0.62
O96555	1Z27	1Z1Y	0.72
Q9X0A5	2EWR	2FCL	0.31
Q97PV8	2HO5	2HO3	0.48
Q87IM6	2QM2	2QHQ	0.47
P0AEH1	3ID2	2ZPM	1.05
Q81VF6	3HA1	2VD8	0.27
Q83Q96	2HKT	3C8G	0.25
Q838I6	2IAC	3BED	0.16
P0A7Z4	1LB2	3K4G	0.79
O05510	1XC3	3OHR	0.25
O58035	2ZZF	2ZZE	0.95
Q6NC90	3DCA	3HHL	0.43
P00447	3BFR	3LSU	0.32
A0KF03	3PSZ	3PSS	0.94
P07550	2R4S	3KJ6	0.51

[#]The RMSD values are calculated using FATCAT structural alignments (53). When the structure is the oligomer, the smallest RMSD value is shown in the list.

Table 4.2. Intermolecular distances between the lysine side-chain Nζ or backbone N atoms of ubiquitin to the nearest heavy atoms of YUH1 or $Dsk2_{UBA}$, calculated from the complex structure[#]

	YUH1 binding		$Dsk2_{UBA}$ binding	
	side-chain Nζ [Å]	backbone N [Å]	side-chain Nζ [Å]	backbone N [Å]
K6	3.9	8.4	3.1 ± 1.0	7.3 ± 0.4
K11	4.9	5.0	13.4 ± 0.5	6.8 ± 0.4
K27	5.2	10.7	11.3 ± 0.6	14.7 ± 0.2
K29	16.9	12.4	21.3 ± 0.6	18.0 ± 0.3
K33	11.5	9.3	19.2 ± 0.6	18.4 ± 0.4
K48	5.0	5.5	5.8 ± 0.7	4.8 ± 0.1
K63	17.6	17.4	17.3 ± 1.2	14.7 ± 0.3

[#]For the YUH1 and $Dsk2_{UBA}$ complexes, crystal (PDB ID: 1CMX) and NMR (PDB ID: 1WR1) structures are available, respectively. For the NMR structure, the distances are calculated for 20 coordinates each with standard deviations.

Table 4.3. Classification between the chemical exchange patterns of the methyl groups and the interaction modes of the lysine side-chains in crystal structures.

	salt bridge[a]	hydrogen bond with backbone[b]	no interaction
split	UBQ K11 UBQ K27[c] FKBP K35 FKBP K47 TRX K18 TRX K96 TRX K100	UBQ K27[d]	TRX K69[e]
broad[c]	FKBP K73 FKBP K105 TRX K3	UBQ K29 TRX K36 TRX K52	—
singlet	—	UBQ K33 TRX K82 TRX K90	UBQ K6 UBQ K48 UBQ K63 FKBP K17 FKBP K34 FKBP K44 FKBP K52 TRX K57[e]

[a] Distance between lysine Nζ atom and the centroid of two O atoms of the nearest carboxyl group is smaller than 4 Å. [b] Distance between lysine Nζ atom and backbone O atom is smaller than 3.5 Å. [c] ^{13}C line width is larger than 20 Hz. [d] Both salt bridge and hydrogen bond with backbone are found. [e] Salt bridge is found in more than half coordinates of the NMR structure ensemble. UBQ, FKBP and TRX indicate ubiquitin, FKBP12 and thioredoxin, respectively.

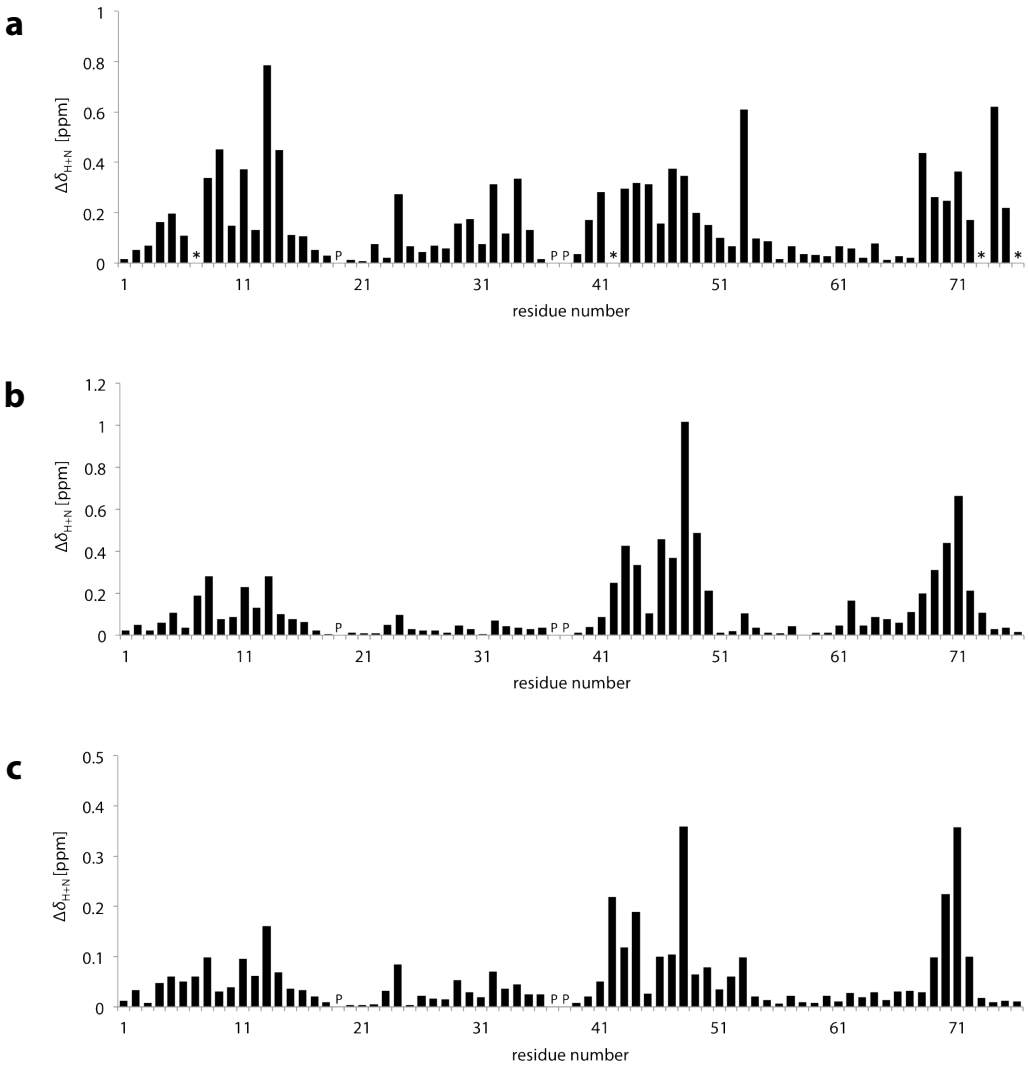

Figure 4.1. ^{1}H and ^{15}N chemical shift changes of *methylated ubiquitin* in the presence of YUH1 (a), $Dsk2_{UBA}$ (b) and $p62_{UBA}$ (c). * and the letter P indicates the unassigned and proline residues, respectively.

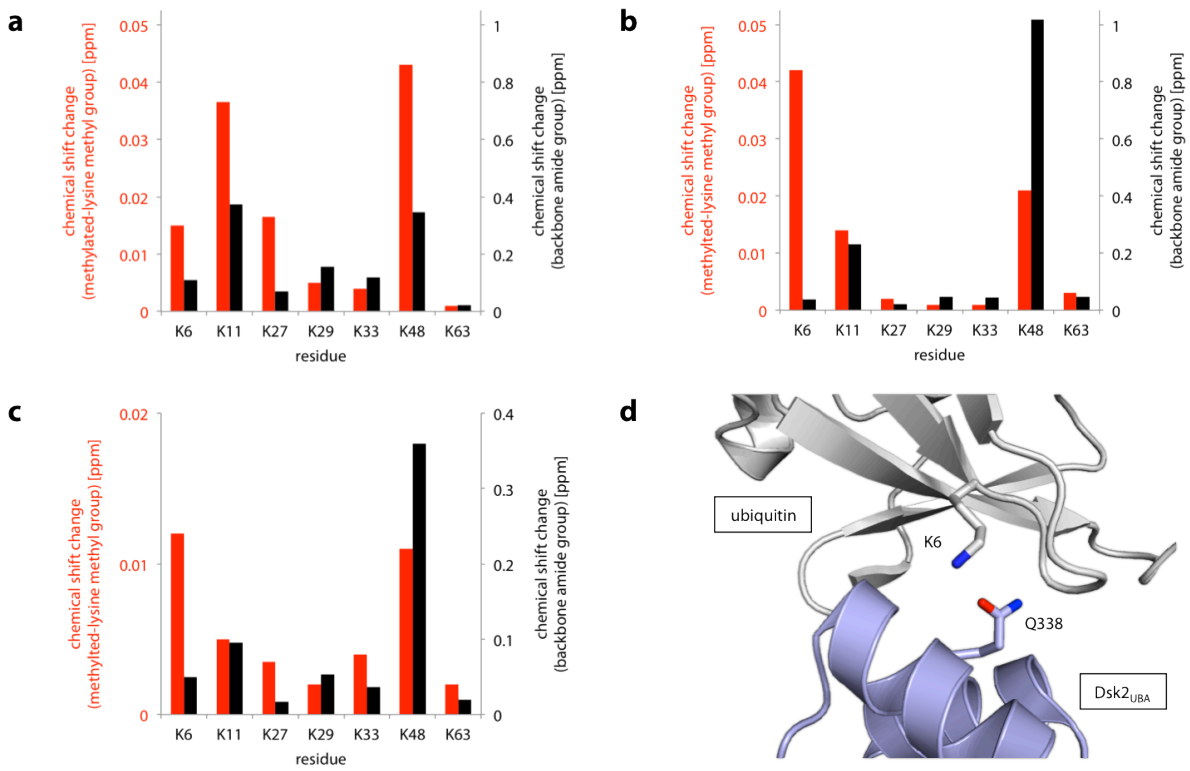

Figure 4.2. Chemical shift changes of lysine methyl groups (red) and backbone amide groups (black) of *methylated-ubiquitin* in the presence of (a) YUH1, (b) $Dsk2_{UBA}$ and (c) $p62_{UBA}$. (d) Enlarged view of Figure 3.5c, where $Dsk2_{UBA}$ colored blue is shown by the ribbon representation instead of surface representation. The side-chains of K6 of ubiquitin and Q338 of $Dsk2_{UBA}$ are shown by the stick representation.

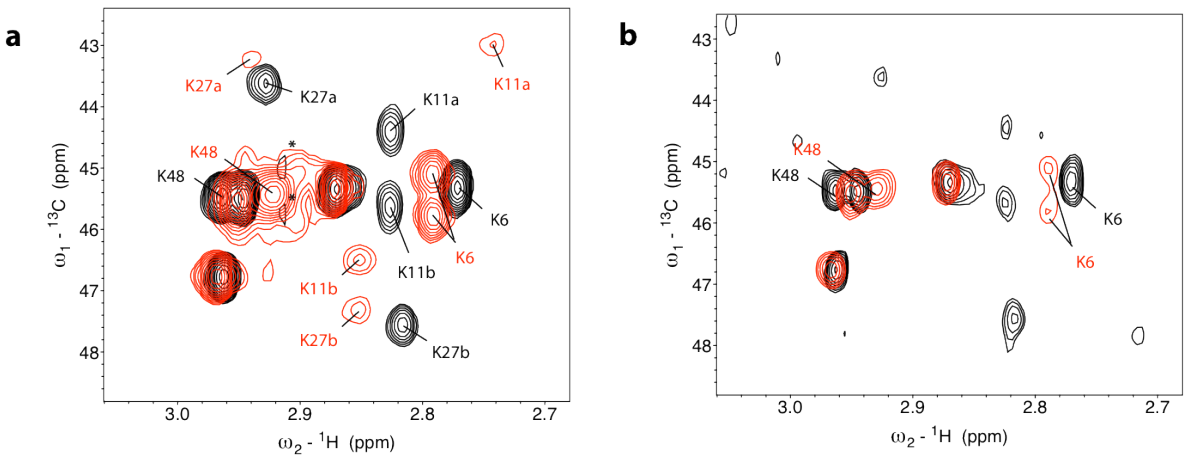

Figure 4.3. Titration experiments by lysine ^{13}C-methylation NMR at low concentration. YUH1 is titrated to *methylated-ubiquitin* and monitored by the methylated-lysine methyl groups. (a) The overlay of the ^{1}H-^{13}C HSQC spectra of 2 μM *methylated ubiquitin* (black) and *methylated ubiquitin* with 10-fold YUH1 (red). * indicates K29. (b) Same as (a) with 0.2 μM *methylated ubiquitin*. All spectra were recorded on 950 MHz NMR.

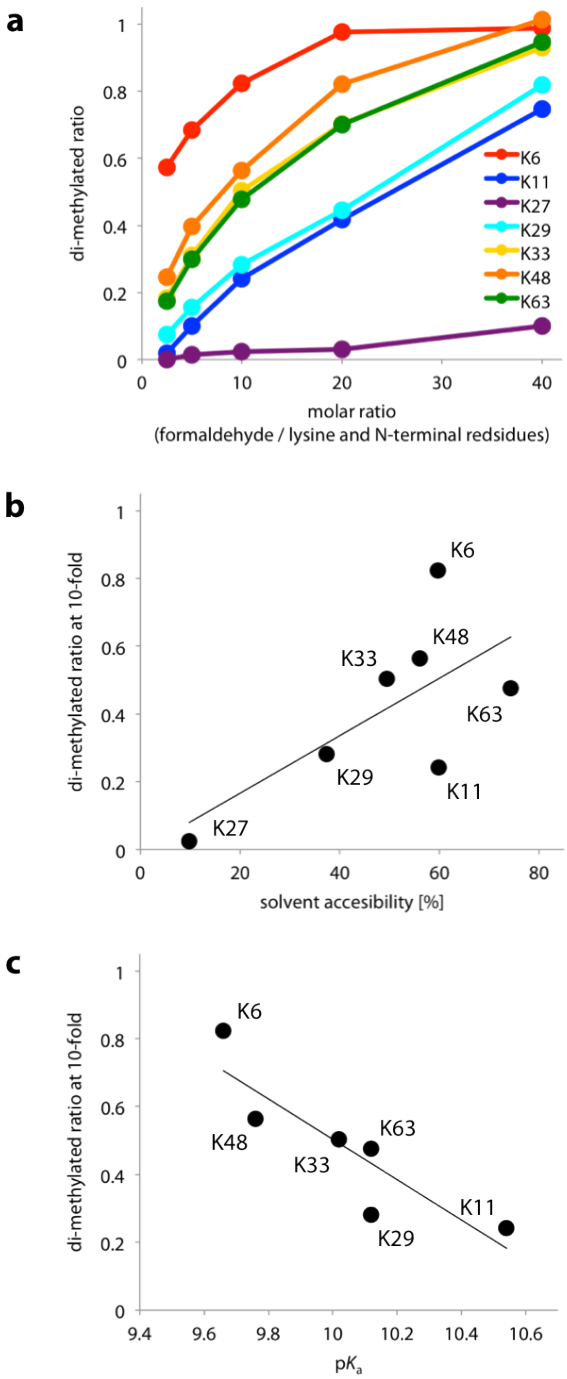

Figure 4.4. (a) The di-methylated ratio against the molar ratio of formaldehyde. The di-methylated ratio is estimated from the peak volumes of the ^{13}C-HSQC spectra. (b) The di-methylated ratio at 20-fold formaldehyde against the solvent accessibility. Least square fitted line is shown. (c) Same as (b) against pK_a value.

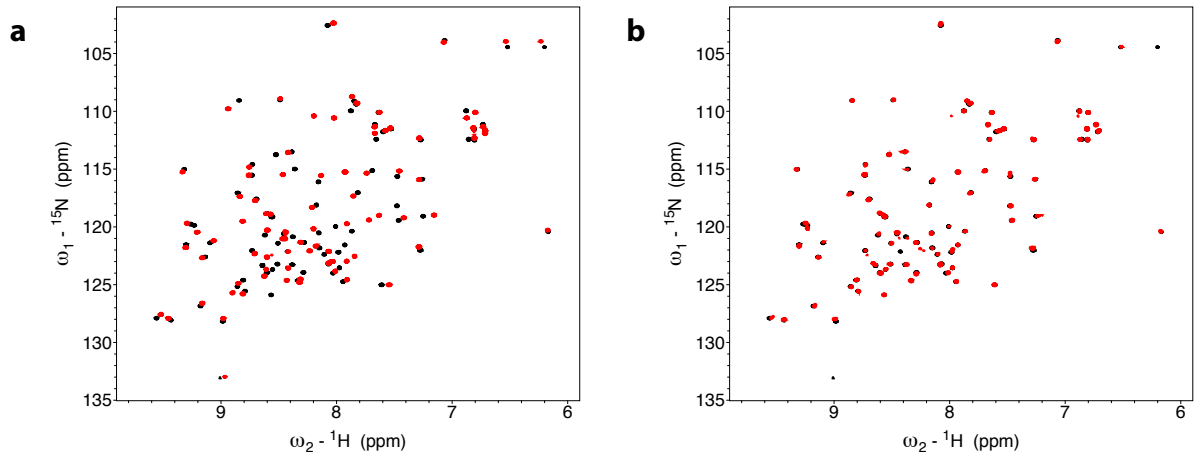

Figure 4.5. The overlay of the ^{1}H-^{15}N HSQC spectra of non-methylated ubiquitin (black) and *methylated ubiquitin* (red). Ubiquitin was methylated using (a) 200-fold or (b) 10-fold of ^{13}C-formaldehyde.

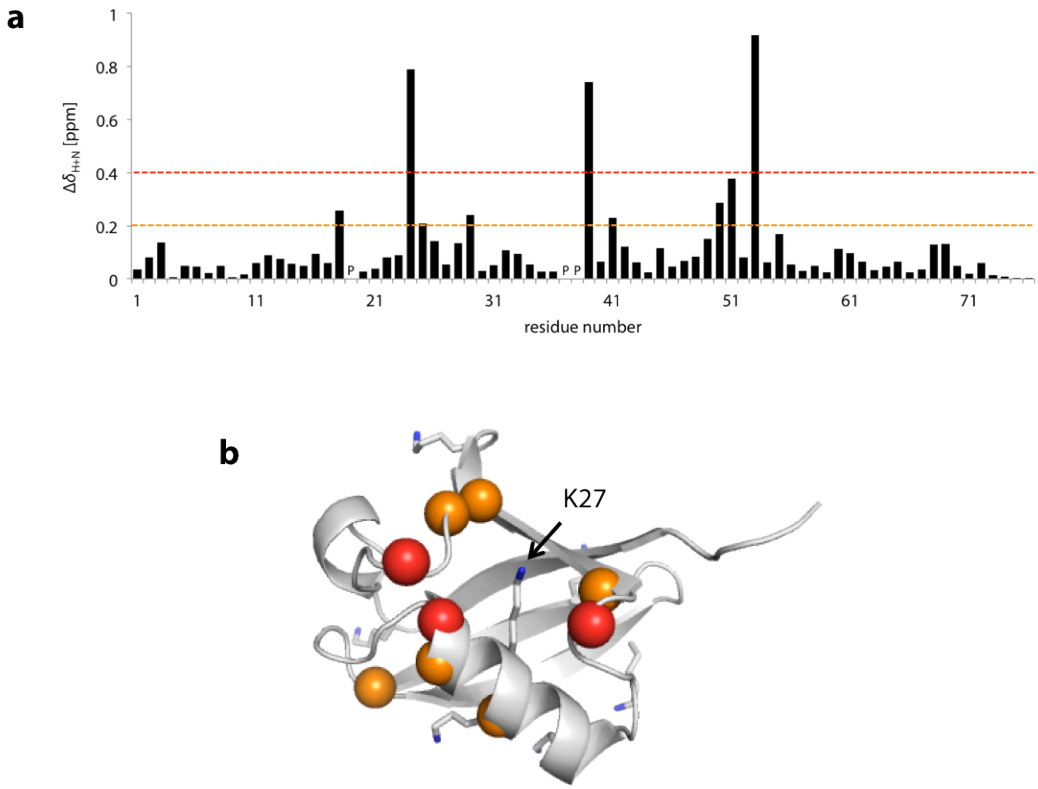

Figure 4.6. ^{1}H and ^{15}N chemical shift changes induced by methylation. (a) The averaged ^{1}H and ^{15}N chemical shift differences between non-methylated ubiquitin and *methylated-ubiquitin*. The letter P indicates the proline residue. (b) Ubiquitin is shown by the ribbon representation. Backbone N atoms with large chemical shift changes are shown by colored spheres. Chemical shift changes within 0.2-0.4 ppm and larger than 0.4 ppm are colored by orange and red, respectively. All lysine residues were drawn by the stick representation.

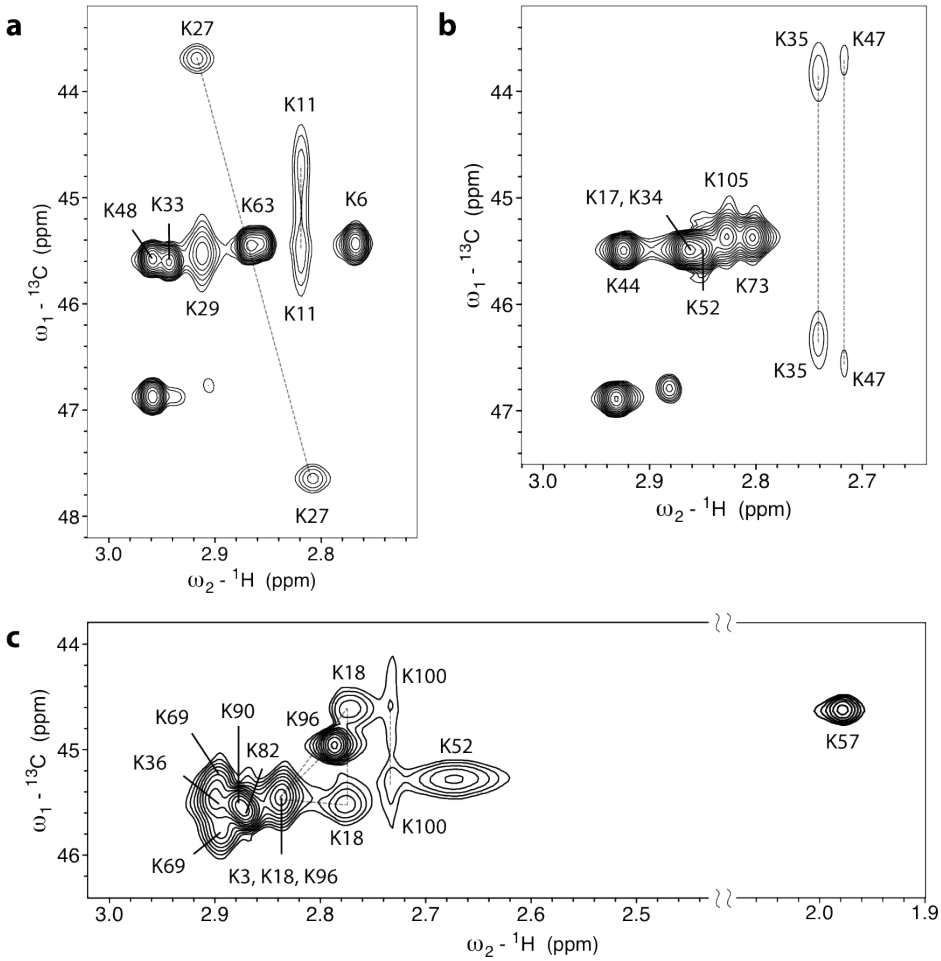

Figure 4.7. ^{1}H-^{13}C HSQC spectra and assignments of methylated (a) ubiquitin, (b) FKBP12 and (c) thioredoxin. These spectra were measured under the same condition; 400 MHz, 303 K and pH 6.8.

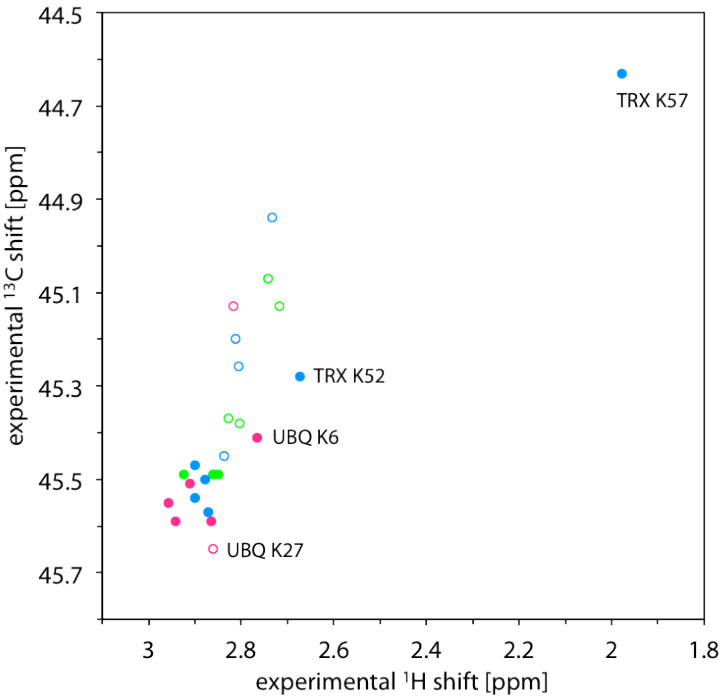

Figure 4.8. Plot between ^{1}H and ^{13}C averaged chemical shifts of the methyl groups. The open circles are "salt bridge" residues as defined in Table 4.3. UBQ, FKBP and TRX indicate ubiquitin, FKBP12 and thioredoxin, respectively. Three proteins were distinguished by colors as UBQ (pink red), FKBP (marine blue) and TRX (light green). UBQ K27 involves not only "salt bridge" but also "hydrogen bond with backbone", and has low solvent accessibility. UBQ K6, TRX K52 and TRX K57 are spatially close to aromatic rings (Nζ atoms are within 6 Å distance from aromatic ring centers).

5. Conclusion

In this study, lysine ^{13}C-methylation NMR was applied to monitor the protein-protein interactions between the ubiquitin and three interacting proteins, YUH1, Dsk2$_{UBA}$, and p62$_{UBA}$. First, the lysine methylation causes little impact on the structure and the protein-protein interaction, revealed by data base survey, ITC, and NMR. Second, the methylated-lysine methyl group is a good probe to monitor the protein-protein interactions and to determine the K_d value. Especially, it is very sensitive to monitor the side-chain interaction. Last, the sensitivity of lysine ^{13}C-methylation NMR is very high, and the protein-protein interactions can be monitored at 0.2-2 μM concentration using the state-of-the-art 950 MHz NMR overnight.

Compared to the conventional NMR methods using ^{15}N-labeled proteins, lysine ^{13}C-methylation has some advantages for probing protein-protein interactions. Lysine ^{13}C-methylation is applicable to the various proteins, which cannot be produced and isotope-labeled using the *E. coli* system, and does not perturb the original protein-protein interaction manner. The chemical shift of the methylated-lysine methyl group, usually locating on the protein surface, shows higher response to the protein-protein interactions than that of the backbone amide group. The NMR sensitivity of the methyl group is much higher than that of the backbone amide groups, which require at least 10 μM concentration. All features of lysine ^{13}C-methylation NMR are suitable for probing protein-protein interactions, and applicable to biologically important larger proteins complexes.

6. Outlook

This study focused on the utilization of NMR analyses using lysine ^{13}C-mehtylation for protein-protein interaction studies. Here the perspectives and the strategies for future analyses are presented.

In application to diluted samples, lysine ^{13}C-methylation is quite useful as this study demonstrated that the 0.2 μM sample was possible to analyze. Indeed, recently, peptide binding to a protein at physiological relevant μM concentration was studied using lysine ^{13}C-methylation (54). The high-sensitivity of lysine ^{13}C-methylation will be also useful for the NMR analysis of high molecular weight proteins, however one major drawback, signal overlap, exists.

NMR signals of the methyl groups appear in the narrow chemical shift range, and the number of lysine residues increases in proportion to the molecular weight. One of the solutions to this problem is increasing pH value. At high pH (about 10), the difference of protonation/deprotonation state of the amino groups generates relatively dispersed NMR spectrum because the pK_a value of amino group is around 10 (19). However, the high pH is not physiologically relevant and the protein is frequently denatured, thus this strategy is not generally applicable. Second solution is to monitor mono-methylated lysine residues. The line width of mono-methylated lysine is significantly narrower than di-methylated lysine mainly due to the absence of exchange process (55). However, the production of mono-methylated lysine is less efficient than di-methylated lysine, and the efficiency depends on the reaction condition. Therefore, the overall sensitivity of mono-methylated lysine is not enough high, and thus more selective mono-methylation reaction scheme needs to be developed. Third solution is producing methyl-lysine analogs by modifying genetically incorporated cysteine or non-natural amino acid (56,57). Although this strategy needs a lot of optimization, it will become useful in site-specific NMR observation of high molecular weight proteins.

In analytical aspect, while the chemical shift perturbation experiments were performed in this study, other approaches could be applied to lysine ^{13}C-methylation. The observation of NOEs for the methyl groups across protein-protein interface is direct evidence of protein-protein interaction and useful for modeling of the complex structure. Cross-saturation method is efficient for more accurate and reliable interface mapping than chemical shift perturbation (58). This method utilizes saturation transfer effect across proteins, and deuteration of a saturation transfer acceptor protein for preventing spin diffusion. The methyl groups in methylated-lysine residues will be useful for the detection probes in acceptor proteins because they are closer to protein interface than backbone atoms.

This study suggests that lysine ^{13}C-methylation is useful for identifying surface-exposed intramolecular salt bridge interaction. This identification relies on chemical shifts and chemical exchanges, and thus they are easy to obtain only by measuring spectra and making assignments. In contrast, conventional NMR analysis could hardly identify surface-exposed salt bridges. This is because the position of solvent-exposed side-chains is generally difficult to be defined due to the lack of NOE distance constraints.

NMR analyses using lysine ^{13}C-methylation will be developed with a central focus on the samples difficult to be labeled by stable isotopes. It will be precious tool for the analyses of diluted and high molecular weight samples utilizing the high sensitivity in NMR measurements. In addition, it will be useful for the analyses of interaction studies, especially in protein-protein interactions, utilizing high responsiveness to the interactions by monitoring side-chain groups close to the protein-protein interfaces. Furthermore, the chemical shifts of the methyl groups are empirically correlated to the surface-exposed salt bridge formation. This relationship will be useful not only for the identification of surface-exposed salt bridges but also for the interpretation of the NMR spectra. These features are fundamental and valuable knowledge for the future progress of the protein NMR analyses.

7. Acknowledgement

This work has been performed under the direction of Prof. Toshimichi Fujiwara, Institute for Protein Research, Osaka University. I would like to express gratitude to the precious advisement and discussion.

I am deeply indebted to Prof. Chojiro Kojima, Institute for Protein Research, Osaka University for the continued guidance to the research.

I am also indebted to Dr. Izuru Ohki, Graduate School of Biological Sciences, Nara Institute of Science and Technology for the precious suggestion and support to the research.

I feel thank to Prof. Takahisa Ikegami and Dr. Kyoko Furuita, Institute for Protein Research, Osaka University for the NMR measurement and analysis, and the discussion about the research. I feel thank to Prof. Harumi Fukada, Graduate School of Life and Environmental Sciences, Osaka Prefecture University for the ITC measurement. I feel thank to Prof. Masahiro Shirakawa, Graduate School of Engineering, Kyoto University for the gift of protein samples. I feel thank to Ms. Momoko Yoneyama, Institute for Protein Research, Osaka University and Ms. Hiroko Kinoshita, Graduate School of Biological Sciences, Nara Institute of Science and Technology for the protein production and constructing the expression system.

I also feel thank to the member in Laboratory of Molecular Biophysics, Institute for Protein Research, Osaka University for the support to the research, and finally I sincerely thank to my family for the continued encouragement.

8. References

1. Ohki, S.Y. and Kainosho, M. (2008) Stable isotope labeling methods for protein NMR spectroscopy. *Progress in Nuclear Magnetic Resonance Spectroscopy*, **53**, 208-226.

2. Sattler, M., Schleucher, J. and Griesinger, C. (1999) Heteronuclear multidimensional NMR experiments for the structure determination of proteins in solution employing pulsed field gradients. *Progress in Nuclear Magnetic Resonance Spectroscopy*, **34**, 93-158.

3. Guntert, P. (2003) Automated NMR protein structure calculation. *Progress in Nuclear Magnetic Resonance Spectroscopy*, **43**, 105-125.

4. Tugarinov, V., Hwang, P.M., Ollerenshaw, J.E. and Kay, L.E. (2003) Cross-correlated relaxation enhanced H-1-C-13 NMR spectroscopy of methyl groups in very high molecular weight proteins and protein complexes. *Journal of the American Chemical Society*, **125**, 10420-10428.

5. Fiaux, J., Bertelsen, E.B., Horwich, A.L. and Wuthrich, K. (2002) NMR analysis of a 900K GroEL-GroES complex. *Nature*, **418**, 207-211.

6. Takahashi, H. and Shimada, I. (2010) Production of isotopically labeled heterologous proteins in non-E. coli prokaryotic and eukaryotic cells. *Journal of Biomolecular NMR*, **46**, 3-10.

7. Means, G.E. and Feeney, R.E. (1968) Reductive alkylation of amino groups in proteins. *Biochemistry*, **7**, 2192-2201.

8. Jentoft, N. and Dearborn, D.G. (1983) Protein labeling by reductive alkylation. *Methods in Enzymology*, **91**, 570-579.

9. Bokoch, M.P., Zou, Y.Z., Rasmussen, S.G.F., Liu, C.W., Nygaard, R., Rosenbaum, D.M., Fung, J.J., Choi, H.J., Thian, F.S., Kobilka, T.S. *et al.* (2010) Ligand-specific regulation of the extracellular surface of a G-protein-coupled receptor. *Nature*, **463**, 108-U121.

10. Williamson, M.P. (2013) Using chemical shift perturbation to characterise ligand binding. *Progress in Nuclear Magnetic Resonance Spectroscopy*, **73**, 1-16.

11. Zuiderweg, E.R.P. (2002) Mapping protein-protein interactions in solution by NMR Spectroscopy. *Biochemistry*, **41**, 1-7.

12. Zhang, M.J. and Vogel, H.J. (1993) Determination of the side-chain pK(a) values of the lysine residues in calmodulin. *Journal of Biological Chemistry*, **268**, 22420-22428.

13. Gerken, T.A. (1984) Amino group environments and metal-binding properties of C-13 reductively methylated bovine alpha-lactalbumin. *Biochemistry*, **23**, 4688-4697.

14. Sherry, A.D. and Teherani, J. (1983) Physical studies of C-13-methylated concanavalin-A - pH-induced and Co2+-induced nuclear magnetic-resonance shifts. *Journal of Biological Chemistry*, **258**, 8663-8669.

15. Dick, L.R., Geraldes, C., Sherry, A.D., Gray, C.W. and Gray, D.M. (1989) C-13 NMR of methylated lysines of fd gene-5 protein - evidence for a conformational change involving lysine-24 upon binding of a negatively charged lanthanide chelate. *Biochemistry*, **28**, 7896-7904.

16. Abraham, S.J., Hoheisel, S. and Gaponenko, V. (2008) Detection of protein-ligand interactions by NMR using reductive methylation of lysine residues. *Journal of Biomolecular NMR*, **42**, 143-148.

17. Jentoft, J.E., Jentoft, N., Gerken, T.A. and Dearborn, D.G. (1979) C-13 NMR-studies of ribonuclease-A methylated with formaldehyde-C-13. *Journal of Biological Chemistry*, **254**, 4366-4370.

18. Brown, L.R. and Bradbury, J.H. (1975) Proton-magnetic-resonance studies of lysine residues of ribonuclease-A. *European Journal of Biochemistry*, **54**, 219-227.

19. Abraham, S.J., Kobayashi, T., Solaro, R.J. and Gaponenko, V. (2009) Differences in lysine pKa values may be used to improve NMR signal dispersion in reductively methylated proteins. *Journal of Biomolecular NMR*, **43**, 239-246.

20. Dick, L.R., Sherry, A.D., Newkirk, M.M. and Gray, D.M. (1988) Reductive methylation and C-13 NMR-studies of the lysyl residues of fd gene 5 protein - lysine-24, lysine-46 and lysine-69 may be involved in nucleic-acid binding. *Journal of Biological Chemistry*, **263**, 18864-18872.

21. Moebius, K., Nordsieck, K., Pichert, A., Samsonov, S.A., Thomas, L., Schiller, J., Kalkhof, S., Pisabarro, M.T., Beck-Sickinger, A.G. and Huster, D. (2013) Investigation of lysine side chain interactions of interleukin-8 with heparin and other glycosaminoglycans studied by a methylation-NMR approach. *Glycobiology*, **23**, 1260-1269.

22. Moore, G.R., Cox, M.C., Crowe, D., Osborne, M.J., Rosell, F.I., Bujons, J., Barker,

P.D., Mauk, M.R. and Mauk, A.G. (1998) N-epsilon,N-epsilon-dimethyl-lysine cytochrome c as an NMR probe for lysine involvement in protein-protein complex formation. *Biochemical Journal*, **332**, 439-449.

23. Funakoshi, M., Sasaki, T., Nishimoto, T. and Kobayashi, H. (2002) Budding yeast Dsk2p is a polyubiquitin-binding protein that can interact with the proteasome. *Proceedings of the National Academy of Sciences of the United States of America*, **99**, 745-750.

24. Ciani, B., Layfield, R., Cavey, J.R., Sheppard, P.W. and Searle, M.S. (2003) Structure of the ubiquitin-associated domain of p62 (SQSTM1) and implications for mutations that cause Paget's disease of bone. *Journal of Biological Chemistry*, **278**, 37409-37412.

25. Ohno, A., Jee, J., Fujiwara, K., Tenno, T., Goda, N., Tochio, H., Kobayashi, H., Hiroaki, H. and Shirakawa, M. (2005) Structure of the UBA domain of Dsk2p in complex with ubiquitin: Molecular determinants for ubiquitin recognition. *Structure*, **13**, 521-532.

26. Isogai, S., Morimoto, D., Arita, K., Unzai, S., Tenno, T., Hasegawa, J., Sou, Y.-s., Komatsu, M., Tanaka, K., Shirakawa, M. *et al.* (2011) Crystal Structure of the Ubiquitin-associated (UBA) Domain of p62 and Its Interaction with Ubiquitin. *Journal of Biological Chemistry*, **286**, 31864-31874.

27. Rayment, I. (1997) Reductive alkylation of lysine residues to alter crystallization properties of proteins. *Methods in Enzymology*, **276**, 171-179.

28. Kay, L.E., Keifer, P. and Saarinen, T. (1992) Pure absorption gradient enhanced heteronuclear single quantum correlation spectroscopy with improved sensitivity. *Journal of the American Chemical Society*, **114**, 10663-10665.

29. Mori, S., Abeygunawardana, C., Johnson, M.O. and Vanzijl, P.C.M. (1995) Improved sensitivity of hsqc spectra of exchanging protons at short interscan delays using a new fast hsqc (FHSQC) detection scheme that avoids water saturation. *Journal of Magnetic Resonance Series B*, **108**, 94-98.

30. Cavanagh, J., Fairbrother, W.J., Palmer, A.G., Rance, M. and Skelton, N.J. (2007) *Protein NMR Spectroscopy, 2nd Edition*. Academic Press, Inc., San Diego.

31. Sakamoto, T., Tanaka, T., Ito, Y., Rajesh, S., Iwamoto-Sugai, M., Kodera, Y., Tsuchida, N., Shibata, T. and Kohno, T. (1999) An NMR analysis of ubiquitin recognition by yeast ubiquitin hydrolase: Evidence for novel substrate recognition by

a cysteine protease. *Biochemistry*, **38**, 11634-11642.

32. Delaglio, F., Grzesiek, S., Vuister, G.W., Zhu, G., Pfeifer, J. and Bax, A. (1995) NMRPipe - A multidimensional spectral processing system based on unix pipes. *Journal of Biomolecular NMR*, **6**, 277-293.

33. Goddard, T.D. and Kneller, D.G. (1999). University of California, San Francisco.

34. Wishart, D.S., Bigam, C.G., Yao, J., Abildgaard, F., Dyson, H.J., Oldfield, E., Markley, J.L. and Sykes, B.D. (1995) H-1, C-13 and N-15 chemical-shift referencing in biomolecular NMR. *Journal of Biomolecular NMR*, **6**, 135-140.

35. Kumar, S. and Nussinov, R. (1999) Salt bridge stability in monomeric proteins. *Journal of Molecular Biology*, **293**, 1241-1255.

36. Kumar, S. and Nussinov, R. (2002) Relationship between ion pair geometries and electrostatic strengths in proteins. *Biophysical Journal*, **83**, 1595-1612.

37. Esadze, A., Li, D.W., Wang, T.Z., Bruschweiler, R. and Iwahara, J. (2011) Dynamics of Lysine Side-Chain Amino Groups in a Protein Studied by Heteronuclear H-1-N-15 NMR Spectroscopy. *Journal of the American Chemical Society*, **133**, 909-919.

38. Gerken, T.A., Jentoft, J.E., Jentoft, N. and Dearborn, D.G. (1982) Intramolecular interactions of amino-groups in C-13 reductively methylated hen egg-white lysozyme. *Journal of Biological Chemistry*, **257**, 2894-2900.

39. Kumar, S. and Nussinov, R. (2002) Close-range electrostatic interactions in proteins. *Chembiochem*, **3**, 604-617.

40. Vijaykumar, S., Bugg, C.E. and Cook, W.J. (1987) Structure of ubiquitin refined at 1.8 Å resolution. *Journal of Molecular Biology*, **194**, 531-544.

41. Baker, E.N. and Hubbard, R.E. (1984) Hydrogen-bonding in globular-proteins. *Progress in Biophysics & Molecular Biology*, **44**, 97-179.

42. Zandarashvili, L., Li, D.W., Wang, T.Z., Bruschweiler, R. and Iwahara, J. (2011) Signature of Mobile Hydrogen Bonding of Lysine Side Chains from Long-Range N-15-C-13 Scalar J-Couplings and Computation. *Journal of the American Chemical Society*, **133**, 9192-9195.

43. Johnston, S.C., Riddle, S.M., Cohen, R.E. and Hill, C.P. (1999) Structural basis for the specificity of ubiquitin C-terminal hydrolases. *Embo Journal*, **18**, 3877-3887.

44. Ofran, Y. and Rost, B. (2003) Analysing six types of protein-protein interfaces. *Journal of Molecular Biology*, **325**, 377-387.

45. Long, J., Garner, T.P., Pandya, M.J., Craven, C.J., Chen, P., Shaw, B., Williamson, M.P., Layfield, R. and Searle, M.S. (2010) Dimerisation of the UBA Domain of p62 Inhibits Ubiquitin Binding and Regulates NF-kappa B Signalling. *Journal of Molecular Biology*, **396**, 178-194.

46. Kay, L.E. (2011) Solution NMR spectroscopy of supra-molecular systems, why bother? A methyl-TROSY view. *Journal of Magnetic Resonance*, **210**, 159-170.

47. Bradbury, J.H. and Brown, L.R. (1973) Determination of dissociation constants of lysine residues of lysozyme by proton-magnetic-resonance spectroscopy. *European Journal of Biochemistry*, **40**, 565-576.

48. Walter, T.S., Meier, C., Assenberg, R., Au, K.F., Ren, J.S., Verma, A., Nettleship, J.E., Owens, R.J., Stuart, D.I. and Grimes, J.M. (2006) Lysine methylation as a routine rescue strategy for protein crystallization. *Structure*, **14**, 1617-1622.

49. Fraczkiewicz, R. and Braun, W. (1998) Exact and efficient analytical calculation of the accessible surface areas and their gradients for macromolecules. *Journal of Computational Chemistry*, **19**, 319-333.

50. Macdonald, J.M., LeBlanc, D.A., Haas, A.L. and London, R.E. (1999) An NMR analysis of the reaction of ubiquitin with acetyl-1-C-13 aspirin. *Biochemical Pharmacology*, **57**, 1233-1244.

52. Buckingham, A.D. (1960) Chemical shifts in the nuclear magnetic resonance spectra of molecules containing polar groups. *Canadian Journal of Chemistry-Revue Canadienne De Chimie*, **38**, 300-307.

53. McConnell, H.M. (1957) Theory of nuclear magnetic shielding in molecules .1. long-range dipolar shielding of protons. *Journal of Chemical Physics*, **27**, 226-229.

54. Ye, Y. and Godzik, A. (2003) Flexible structure alignment by chaining aligned fragment pairs allowing twists. *Bioinformatics*, **19**, II246-II255.

55. Chavan, T.S., Abraham, S. and Gaponenko, V. (2013) Application of Reductive C-13-Methylation of Lysines to Enhance the Sensitivity of Conventional NMR Methods. *Molecules*, **18**, 7103-7119.

56. Larda, S.T., Bokoch, M.P., Evanics, F. and Prosser, R.S. (2012) Lysine methylation

strategies for characterizing protein conformations by NMR. *Journal of Biomolecular NMR*, **54**, 199-209.

57. Cui, G.F., Botuyan, M.V. and Mer, G. (2009) Preparation of Recombinant Peptides with Site- and Degree-Specific Lysine C-13-Methylation. *Biochemistry*, **48**, 3798-3800.

58. Guo, J.T., Wang, J.Y., Lee, J.S. and Schultz, P.G. (2008) Site-specific incorporation of methyl- and acetyl-lysine analogues into recombinant proteins. *Angewandte Chemie-International Edition*, **47**, 6399-6401.

59. Shimada, I., Ueda, T., Matsumoto, M., Sakakura, M., Osawa, M., Takeuchi, K., Nishida, N. and Takahashi, H. (2009) Cross-saturation and transferred cross-saturation experiments. *Progress in Nuclear Magnetic Resonance Spectroscopy*, **54**, 123-140.